Available online at www.sciencedirect.com

ScienceDirect

Journal of the Franklin Institute 355 (2018) 6780–6809

www.elsevier.com/locate/jfranklin

Fixed-time synchronization of memristor-based fuzzy cellular neural network with time-varying delay☆

Mingwen Zheng[a,b], Lixiang Li[c,*], Haipeng Peng[c], Jinghua Xiao[b,d], Yixian Yang[c], Yanping Zhang[a], Hui Zhao[e]

[a] *School of Mathematics and Statistics, Shandong University of Technology, Zibo 255000, China*

[b] *School of Science, Beijing University of Posts and Telecommunications, Beijing 100876, China*

[c] *Information Security Center, State Key Laboratory of Networking and Switching Technology, Beijing University of Posts and Telecommunications, Beijing 100876, China*

[d] *State Key Laboratory of Information Photonics and Optical Communications, Beijing University of Posts and Telecommunications, Beijing 100876, China*

[e] *Shandong Provincial Key Laboratory of Network Based Intelligent Computing, School of Information Science and Engineering, University of Jinan, Jinan 250022, China*

Received 11 August 2017; received in revised form 5 March 2018; accepted 24 June 2018
Available online 10 July 2018

Abstract

This paper mainly investigates the fixed-time synchronization of memristor-based fuzzy cellular neural network (MFCNN) with time-varying delay. By utilizing differential inclusion, set-valued map theory, the definitions of finite-time and fixed-time stability, we convert the fixed-time synchronization control of the drive-response MFCNN into the equivalent fixed-time stability problem of the error system between the drive-response systems. Some novel sufficient conditions are derived to guarantee the fixed-time synchronization of the drive-response MFCNN based on a simple Lyapunov function and a nonlinear feedback controller. Meanwhile, the settling time can be estimated by simple calculations. Furthermore, these fixed-time synchronization criteria here are easy to validate and extend to the MFCNN without time-varying delay and general memristor-based neural networks. Finally, three numerical examples are given to illustrate the correctness of the main results.

☆ This paper is supported by the National Key R&D Program of China (Grant No. 2016YFB0800602), the National Natural Science Foundation of China (Grant Nos. 61472045, 61573067), the Natural Science Foundation of Shandong Province (Grant No. ZR2018BF023).

* Corresponding author.
E-mail address: li_lixiang2006@163.com (L. Li).

https://doi.org/10.1016/j.jfranklin.2018.06.041

1. Introduction

Cellular neural network (CNN) was pioneered by Chua and Yang [1]. Compared with the traditional artificial neural network, the characteristics of neuron connections in CNN make it easy to be implemented in very large scale integrated circuits (VLSI). Therefore, it is widely used in pattern recognition, dynamic image processing, associative memory, partial differential equation numerical solution, combinatorial optimization, etc [2–10]. But the standard CNN has linearly weighted connections and cannot implement nonlinear filtering. The feature limits the applications of it. In 1996, Yang and Yang proposed the fuzzy cellular neural network (FCNN) by introducing two fuzzy operators, namely "fuzzy AND ($\bigwedge$)" and "fuzzy OR ($\bigvee$)". It is found that FCNN has better applications in image processing and pattern recognition [11–14].

Chua postulated a new basic circuit element named memristor, a combination of memory and resistor, between charge and flux when he studied the relationships between charge, current, voltage and flux in 1971 [15]. However, the real memristor was developed by the researchers at the Hewlett-Packard lab [16] until 2008. The memristor is a nonlinear resistor with memory function. Its resistance is not a constant and can be changed by the current flowing through it. Because the nano-scale, low energy consumptions and nonvolatile characteristics of the memristor, the information can be stored and processed well. Some studies show that the memristor can exhibit pinched hysteresis, which is very similar to the transmission mode between synapses [17]. Extensive research shows that the neuromorphic computing method composed of memristors is likely to break through the bottleneck of Von-Neumann computer architecture [18,19]. As we know, the traditional hardware-implemented artificial neural networks adopt resistors to simulate synapses, which is the key part of information transmission between neurons. But it becomes increasingly difficult to reduce resistor dimensions [20]. Because of the unique characteristics, the memristor has become the best device to simulate synapses at present. Many scholars have studied various memristor-based neural network models from the theories and applications [21–27]. Combining memristor and FCNN to form memristor-based fuzzy neural networks (MFCNN), it seems that no one has studied the MFCNN. This is one of the motivations of our paper.

As one of the main research contents of neural network dynamics, the stability problem of neural network has been paid more and more attention. And as an application of the stability of neural network, the synchronization control of neural network is often transformed into the stability problem of the corresponding error system. The synchronization control of neural network originated from the chaotic system synchronization between the drive and response systems with different initial values, which was proposed by Pecora and Carroll [28]. Considering the time to reach synchronization, the neural network synchronization mainly includes asymptotic synchronization, finite-time synchronization and fixed-time synchronization. Different from the asymptotical synchronization, finite-time synchronization and the fixed-time synchronization require that the trajectories of the drive-response systems achieve synchronization after a finite-time interval. The finite-time synchronization of the system is one of the applications of finite-time stability, which was first presented by Kamenkov in 1953 [29]. Fixed-time stability first proposed by Polyakov [30], can be seen as a special case of finite-time stability. Both finite-time stability and fixed-time stability mean that the system can achieve convergence over a finite time interval. The main difference between them is that the convergence time or settling time (denoted by $T(x_0)$) of the finite-time stability is related to the initial values of the system, while the settling time (denoted by T_{max}) of fixed-time

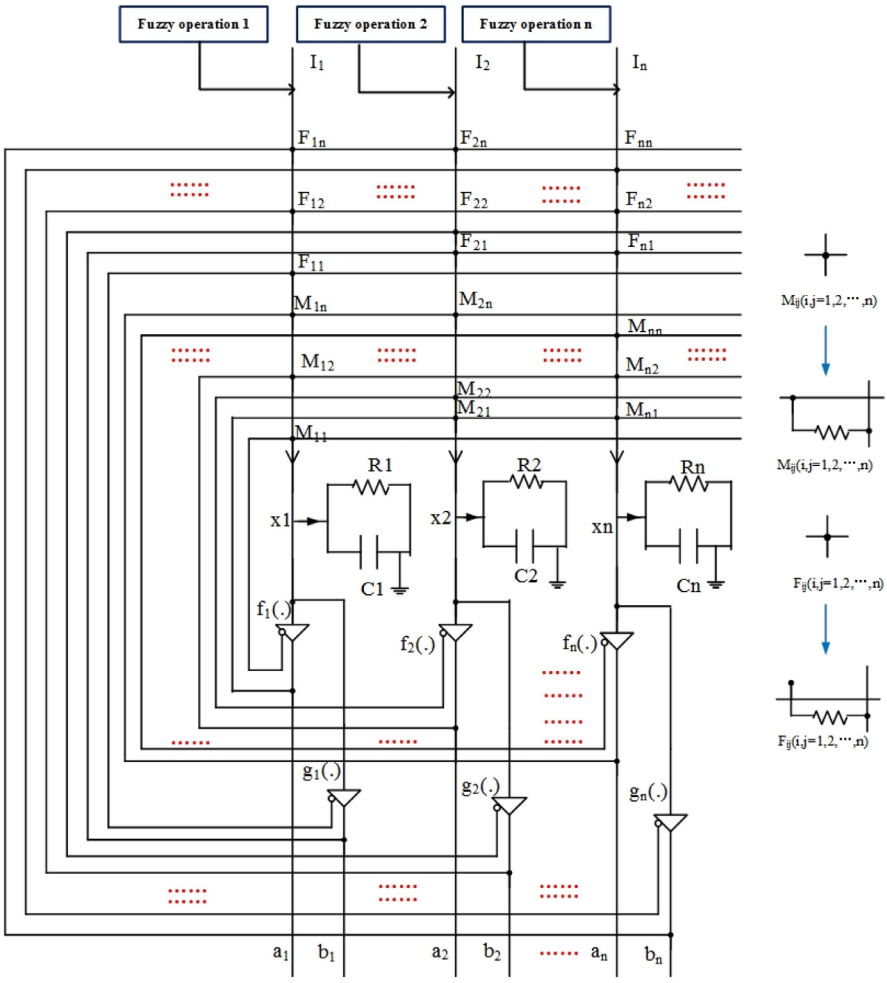

Fig. 1. The circuit schematic diagram of the MFCNN.

stability has a uniform upper bound for all initial values within the domain. And there is $T(x_0) \leq T_{max}$. In the synchronous control problem, the estimation of the $T(x_0)$ or T_{max} is one of the key issues. According to the definition of finite-time synchronization, we know that the $T(x_0)$ depends on the initial values of the system, in other words, different initial conditions will get different $T(x_0)$. But in the real control system, the initial conditions are not easy to obtain. Obviously, finite-time synchronization is not very suitable for some practical applications where the $T(x_0)$ must be determined for any initial conditions. Fortunately, fixed-time synchronization overcomes this problem. The settling time (T_{max}) of fixed-time synchronization is independent of the initial values of the system. Many practical systems, such as traffic signals [31] and power systems [32], must be controlled in a fixed time. Therefore, it is meaningful and valuable to study the fixed-time synchronization control. In this paper, we will study the fixed-time synchronization control problem of the MFCNN because of the few current theoretical results. This is another research motivation of our work.

Compared with many finite-time problems [33–38], the research of fixed-time stability or synchronization is still in a primitive stage. Polyakov et al. designed new nonlinear control laws for robust stabilization of nonlinear systems based on the finite-time and fixed-time stability theorems utilizing an implicit Lyapunov function [39]. Cao et al. investigated the fixed-time synchronization of master-slave Cohen-Grossberg neural networks, and proposed novel synchronization criteria by the Lyapunov stability theory [40]. In Ref. [41], Liu et al. revealed the essence of finite-time and fixed-time stability by treating finite-time stability as an inverse problem, and gave some necessary and sufficient conditions. Liu and Chen studied the finite-time and fixed-time cluster synchronization of complex networks with or without pinning control. They also designed some simple distributed protocols, and obtained several sufficient criteria to ensure cluster synchronization [42]. In the existing literatures related to fuzzy neural networks, Ref. [43] discussed the exponentially lag synchronization of fuzzy cellular neural networks with time-varying delays. Ref. [44] investigated the asymptotical synchronization of no-identical chaotic fuzzy cellular neural networks with time-varying delays based on sliding mode control. Abdurahman et al. studied the finite-time synchronization of fuzzy cellular neural networks with time-varying delays [45]. Including the delays, there are also some studies of the impact of other types of constraints on synchronization. Ref. [46] investigated pinning synchronization of Takagi–Sugeno fuzzy complex network with partial couplings (only partial node information available) and discrete-time couplings (nodes' sample information available) for the first time. These results overcome the difficulty of less effective information for synchronization. Lu et al. discussed outer synchronization of drive-response partially coupled dynamical networks utilizing pinning impulsive controller [47]. Ref. [48] investigated the periodicity and synchronization of the time-varying coupled memristive neural networks with supremums in the activation function, and novel criteria are derived to guarantee the synchronization based on new $\omega-$matrix measure approach. Recently, Wang et al. studied the sampled-data cluster formation for nonlinear multi-agent systems via the event-triggered sampling [49].

However, in the above results, there is no literature to study the fixed-time synchronization problem of fuzzy neural networks and the network model does not contain the memristor. There are two difficulties in the study of fixed-time synchronization of the MFCNN. Firstly, because of the existence of the memristor, the MFCNN becomes differential equations with discontinuous right-hand sides. How to transform it into continuous differential equations is a problem to overcome. Second, how to design simple fixed-time synchronization controllers is also a challenge. To sum up, considering the fact that there is almost no literature about fixed-time synchronization of MFCNN and the important influence of delays on the stability of system [50], these have become the main motivation for our study of fixed-time synchronization of the drive-response MFCNN with time-varying delays.

The memristor-based neural network has the characteristics of inherent switching subsystems and local range motion uncertainty, and the addition of fuzzy logic causes more complicated dynamic behavior. Inspired by the above discussions, the main goal of this paper is to investigate the fixed-time synchronization of the MFCNN with time-varying delay under the framework of Filippov solution by utilizing differential inclusions, set-valued map, finite-time stability and fixed-time stability theory. The main contributions of this paper are summarized below.

(1) The neural network model (MFCNN) discussed in this paper includes memristor model, fuzzy logic and time-varying delays simultaneously. The MFCNN is more complex and

more general than the conventional neural networks. Therefore, the theoretical results of this paper are more general.

(2) The fixed-time synchronization problem of drive-response MFCNN with time-varying delays is discussed for the first time. Fixed-time synchronization is more practical than the asymptotic synchronization and the finite-time synchronization in some practical applications.

(3) A simple fixed-time synchronization controller is designed and some sufficient conditions for easy verification are obtained to guarantee the fixed-time synchronization of drive-response MFCNN. Moreover, the settling time (T_{max}) can be easily estimated.

The rest of this paper is organized as follows. In Section 2, the differential inclusions, set-valued map, MFCNN model, fixed-time synchronization, some definitions and lemmas are introduced. We derive the several sufficient conditions of fixed-time synchronization between the drive-response MFCNN with time-varying delay in Section 3. Three numerical examples show the effectiveness of our theoretical results in Section 4. Finally, We summarize this paper and put forward the future works in Section 5.

2. Preliminaries

In this section, we will give the mathematical model of the memristor-based fuzzy cellular neural network with time-varying delay first. Then some assumptions, definitions, and lemmas will be introduced to derive the main results.

2.1. The drive-response MFCNN Models

The memristor-based fuzzy cellular neural network with time-varying delay in this paper is as follows:

$$\begin{cases} \dot{x}_i(t) = -c_i x_i(t) + \sum\limits_{j=1}^{n} \tilde{a}_{ij}(x_j(t)) f_j(x_j(t)) + \sum\limits_{j=1}^{n} \tilde{b}_{ij}(x_j(t-\tau_j(t))) g_j(x_j(t-\tau_j(t))) \\ \qquad + \sum\limits_{j=1}^{n} d_{ij} v_j + \bigwedge\limits_{j=1}^{n} T_{ij} v_j + \bigwedge\limits_{j=1}^{n} \alpha_{ij} g_j(x_j(t-\tau_j(t))) + \bigvee\limits_{j=1}^{n} S_{ij} v_j \\ \qquad + \bigvee\limits_{j=1}^{n} \beta_{ij} g_j(x_j(t-\tau_j(t))) + I_i, \\ x_i(t) = \phi_i(t), t \in [-\tau, 0], i = 1, 2, \ldots, n, \end{cases} \tag{1}$$

where $x_i(t)$ represents the state variable of the ith neuron at time t; c_i denotes the passive decay rates to the ith neuron; d_{ij}, T_{ij}, α_{ij}, β_{ij}, S_{ij} are elements of feed-forward template, fuzzy feed-forward MIN template, fuzzy feedback MIN template, fuzzy feedback MAX template and fuzzy Feed-forward MAX template, respectively. v_j denotes the input of the jth neuron; I_i is the bias value of the ith neuron; $\tau_j(t)$ is the time-varying delay; f_i, g_i are the ith activation functions. $\phi_i(t) \in C([-\tau, 0], \mathbb{R})$ is the initial value of the model (1), where $\tau = \max_j\{\tau_j(t)\}$, $C([-\tau, 0], \mathbb{R})$ represents a continuous function set from the interval $[-\tau, 0]$ to $\mathbb{R}$; $\tilde{a}_{ij}(x_j(t))$ and $\tilde{b}_{ij}(x_j(t-\tau_j(t)))$ denote the non-delayed and delayed memristor-based synaptic

connection weights, respectively. $\tilde{a}_{ij}$ and $\tilde{b}_{ij}$ are defined as follows

$$\tilde{a}_{ij}(x_j(t)) = \begin{cases} \tilde{a}_{ij}^{(1)}, |x_j(t)| \le T_j, \\ \tilde{a}_{ij}^{(2)}, |x_j(t)| > T_j, \end{cases}$$

$$\tilde{b}_{ij}(x_j(t-\tau_j(t))) = \begin{cases} \tilde{b}_{ij}^{(1)}, |x_j(t-\tau_j(t))| \le T_j, \\ \tilde{b}_{ij}^{(2)}, |x_j(t-\tau_j(t))| > T_j, \end{cases}$$

where where T_j is the switching jump, $\tilde{a}_{ij}^{(1)}, \tilde{a}_{ij}^{(2)}, \tilde{b}_{ij}^{(1)}, \tilde{b}_{ij}^{(2)}, i, j = 1, 2, \ldots, n$ are all constant numbers.

Remark 1. $\bigvee$ and $\bigwedge$ denote the fuzzy AND operation (take the minimum) and fuzzy OR operation (take the maximum), respectively. In the fuzzy cellular neural networks, the matrix composed of each set of connection parameters is called a template. The feed-forward template refers to the connection parameters of the two neurons at time t, while the feedback template refers to the delay connection parameters of the two neurons at time $t-\tau$. Thus, the feedback MIN template represents the connection parameters with the fuzzy AND operation; the feedback MAX template represents the connection parameters with the fuzzy OR operation; fuzzy feed-forward MIN template represents the delay connection parameters with the fuzzy AND operation; and fuzzy feed-forward MAX template represents the delay connection parameters with the fuzzy OR operation.

Remark 2. By referring to the existing literature [51,52], we draw the circuit schematic diagram (Fig. 1). The weights of the MFCNN consist of memristors, and the resistance of the memristor can be changed according to the system states. So the MFCNN can be regarded as a special switched neural network system. FCNN is not a switched system. This is the main difference between the MFCNN and the FCNN.

From the definitions of $\tilde{a}_{ij}(x_j(t))$ and $\tilde{b}_{ij}(x_j(t-\tau_j(t)))$, the model (1) is a switching differential equation with discontinuous right-hand sides. For this kind of equation, Filippov had given an effective treatment approach [53,54]. In order to facilitate the handling of this type of equation, we define the set-valued maps

$$K\left[\tilde{a}_{ij}(x_j(t))\right] = \begin{cases} \tilde{a}_{ij}^{(1)}, |x_j(t)| < T_j, \\ \overline{co}\{\underline{a}_{ij}, \overline{a}_{ij}\}, |x_j(t)| = T_j, \\ \tilde{a}_{ij}^{(2)}, |x_j(t)| > T_j, \end{cases}$$

$$K\left[\tilde{b}_{ij}(x_j(t-\tau_j(t)))\right] = \begin{cases} \tilde{b}_{ij}^{(1)}, |x_j - \tau_j(t)| < T_j, \\ \overline{co}\left\{\underline{b}_{ij}, \overline{b}_{ij}\right\}, |x_j\left(t-\tau_j(t)\right)| = T_j, \\ \tilde{b}_{ij}^{(2)}, |x_j\left(t-\tau_j\right)| > T_j, \end{cases}$$

where $\underline{a}_{ij} = \min\left\{\tilde{a}_{ij}^{(1)}, \tilde{a}_{ij}^{(2)}\right\}$, $\overline{a}_{ij} = \max\left\{\tilde{a}_{ij}^{(1)}, \tilde{a}_{ij}^{(2)}\right\}$, $\underline{b}_{ij} = \min\left\{\tilde{b}_{ij}^{(1)}, \tilde{b}_{ij}^{(2)}\right\}$, $\overline{b}_{ij} = \max\left\{\tilde{b}_{ij}^{(1)}, \tilde{b}_{ij}^{(2)}\right\}$, $\overline{co}$ denotes the convex closure of a set and $K\left[\tilde{a}_{ij}(x_j(t))\right], K\left[\tilde{b}_{ij}(x_j(t-\tau_j(t)))\right]$ are all closed, convex and compact about $x_j(t), x_j(t-\tau_j(t))$.

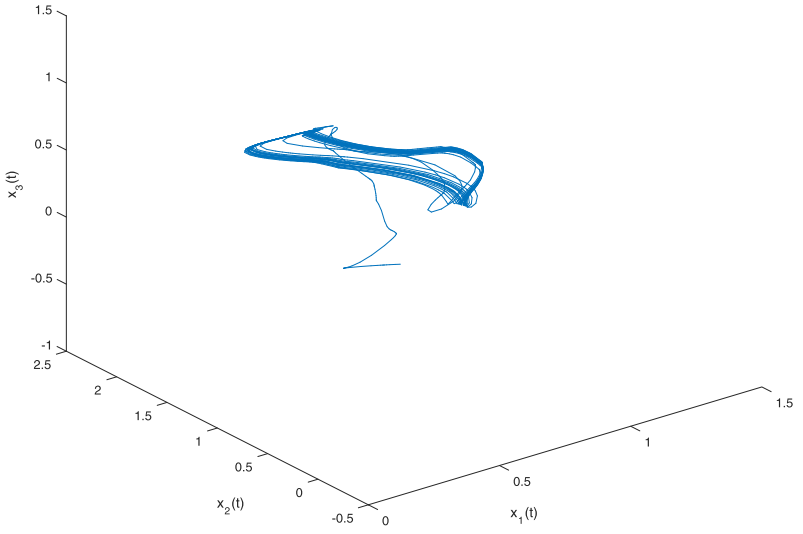

Fig. 2. The phase diagram of the drive system in (20) when the initial value $\phi(t) = [0.2 + 0.1sin(t); -0.4 + 0.1cos(t); 0.6 + 0.1sin(t)]$.

With the help of the differential inclusions theory, the model (1) can be rewritten as

$$\begin{aligned}\dot{x}_i(t) \in -c_i x_i(t) + \sum_{j=1}^{n} K\big[\tilde{a}_{ij}(x_j(t))\big] f_j(x_j(t)) + \sum_{j=1}^{n} K\Big[\tilde{b}_{ij}\big(x_j\big(t-\tau_j(t)\big)\big)\Big] g_j\big(x_j(t-\tau_j(t))\big) \\ + \sum_{j=1}^{n} d_{ij} v_j + \bigwedge_{j=1}^{n} T_{ij} v_j + \bigwedge_{j=1}^{n} \alpha_{ij} g_j\big(x_j(t-\tau_j(t))\big) \\ + \bigvee_{j=1}^{n} S_{ij} v_j + \bigvee_{j=1}^{n} \beta_{ij} g_j\big(x_j(t-\tau_j(t))\big) + I_i, \end{aligned} \tag{2}$$

According to the measurable selection theorem [55], there exist measurable functions $\hat{a}_{ij}(t) \in K\big[\tilde{a}_{ij}(x_j(t))\big]$, $\hat{b}_{ij} \in K\Big[\tilde{b}_{ij}(t)(x_j(t-\tau_j(t)))\Big]$ for a.e. $t \geq 0$ such as

$$\begin{aligned}\dot{x}_i(t) = -c_i x_i(t) + \sum_{j=1}^{n} \hat{a}_{ij}(t) f_j(x_j(t)) + \sum_{j=1}^{n} \hat{b}_{ij}(t) g_j\big(x_j\big(t-\tau_j(t)\big)\big) + \sum_{j=1}^{n} d_{ij} v_j \\ + \bigwedge_{j=1}^{n} T_{ij} v_j + \bigwedge_{j=1}^{n} \alpha_{ij} g_j\big(x_j(t-\tau_j(t))\big) + \bigvee_{j=1}^{n} S_{ij} v_j + \bigvee_{j=1}^{n} \beta_{ij} g_j\big(x_j(t-\tau_j(t))\big) + I_i. \end{aligned} \tag{3}$$

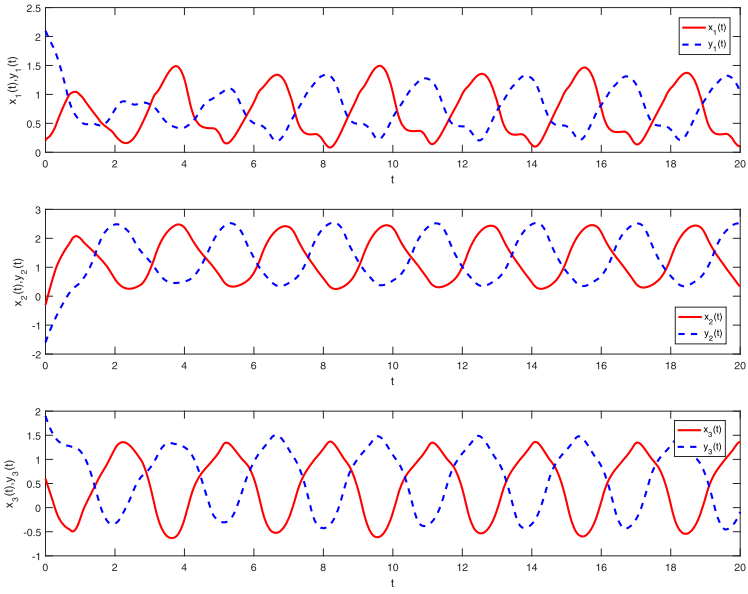

Fig. 3. The trajectories of drive-response system (20) without the controller.

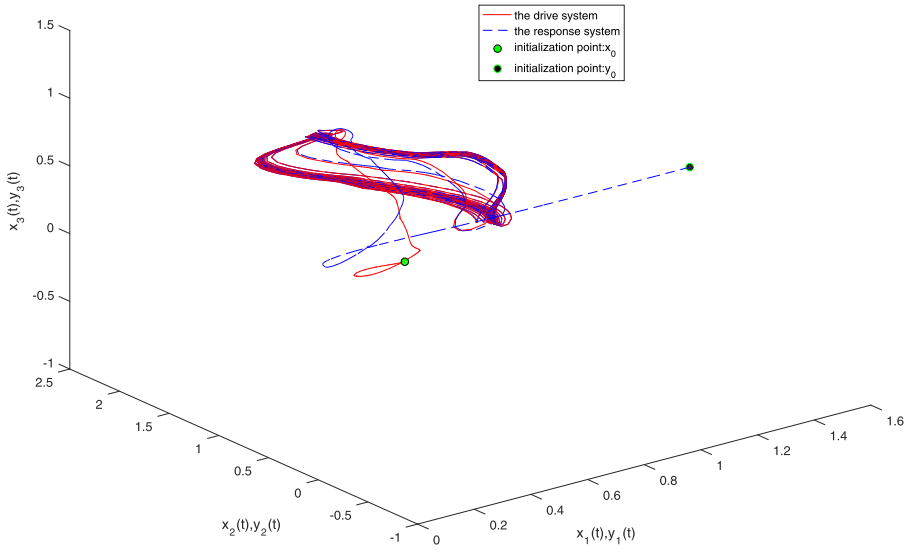

Fig. 4. The phase diagram and the initialization points of the drive-response systems (20) with controller.

Let the MFCNN (1) be the drive system. The corresponding response system is selected as follows:

$$\begin{cases} \dot{y}_i(t) = -c_i y_i(t) + \sum_{j=1}^{n} \tilde{a}_{ij}(y_j(t)) f_j(y_j(t)) + \sum_{j=1}^{n} \tilde{b}_{ij}\big(y_j(t-\tau_j(t))\big) g_j\big(y_j(t-\tau_j(t))\big) + \sum_{j=1}^{n} d_{ij} v_j \\ \qquad + \bigwedge_{j=1}^{n} T_{ij} v_j + \bigwedge_{j=1}^{n} \alpha_{ij} g_j\big(y_j(t-\tau_j(t))\big) + \bigvee_{j=1}^{n} S_{ij} v_j + \bigvee_{j=1}^{n} \beta_{ij} g_j\big(y_j(t-\tau_j(t))\big) + I_i + u_i(t), \\ y_i(t) = \varphi_i(t), t \in [-\tau, 0], i = 1, 2, \ldots, n, \end{cases} \tag{4}$$

where $u_i(t)$ a fixed-time synchronization controller to be defined, $\tilde{a}_{ij}(y_j(t))$ and $\tilde{b}_{ij}(y_j(t-\tau_j(t)))$ are as follows

$$\tilde{a}_{ij}(y_j(t)) = \begin{cases} \tilde{a}_{ij}^{(1)}, |y_j(t)| \le T_j, \\ \tilde{a}_{ij}^{(2)}, |y_j(t)| > T_j, \end{cases}$$

$$\tilde{b}_{ij}(y_j(t-\tau_j(t))) = \begin{cases} \tilde{b}_{ij}^{(1)}, |y_j(t-\tau_j(t))| \le T_j, \\ \tilde{b}_{ij}^{(2)}, |y_j(t-\tau_j(t))| > T_j, \end{cases}$$

Similarly, we have

$$K\big[\tilde{a}_{ij}(y_j(t))\big] = \begin{cases} \tilde{a}_{ij}^{(1)}, |y_j(t)| < T_j, \\ \overline{co}\{\underline{a}_{ij}, \overline{a}_{ij}\}, |y_j(t)| = T_j, \\ \tilde{a}_{ij}^{(2)}, |y_j(t)| > T_j, \end{cases}$$

$$K\Big[\tilde{b}_{ij}(y_j(t-\tau_j(t)))\Big] = \begin{cases} \tilde{b}_{ij}^{(1)}, |y_j - \tau_{ij}(t)| < T_j, \\ \overline{co}\{\underline{b}_{ij}, \overline{b}_{ij}\}, |y_j(t-\tau_j(t))| = T_j, \\ \tilde{b}_{ij}^{(2)}, |y_j\big(t-\tau_j(t)\big)| > T_j, \end{cases}$$

$K\big[\tilde{a}_{ij}(y_j(t))\big], K\Big[\tilde{b}_{ij}(y_j(t-\tau_j(t)))\Big]$ are also all closed, convex and compact about $y_j(t)$ and $y_j(t-\tau_j(t))$, respectively.

Similarly, There exist measurable functions $\breve{a}_{ij}(t) \in K[\tilde{a}_{ij}(y_j(t))]$, $\breve{b}_{ij} \in K[\tilde{b}_{ij}(t)(y_j(t-\tau_j(t)))]$ for a.e. $t \ge 0$ such as

$$\begin{aligned} \dot{y}_i(t) = -c_i y_i(t) + \sum_{j=1}^{n} \breve{a}_{ij}(t) f_j(y_j(t)) + \sum_{j=1}^{n} \breve{b}_{ij}(t) g_j\big(y_j(t-\tau_j(t))\big) + \sum_{j=1}^{n} d_{ij} v_j \\ + \bigwedge_{j=1}^{n} T_{ij} v_j + \bigwedge_{j=1}^{n} \alpha_{ij} g_j(y_j\big(t-\tau_j(t)\big)) + \bigvee_{j=1}^{n} S_{ij} v_j + \bigvee_{j=1}^{n} \beta_{ij} g_j\big(y_j(t-\tau_j(t))\big) + I_i + u_i(t). \end{aligned} \tag{5}$$

For the drive-response systems (1) and (4), we have the following assumption.

Assumption 1. The activation functions $f_i(x)$, $g_i(x)$ are Lipschitz continuous on $\mathbb{R}$, i.e., there exist positive constants l_i, m_i that make the following inequality hold

$$|f_i(y) - f_i(x)| \le l_i|y - x|,$$
$$|g_i(y) - g_i(x)| \le m_i|y - x|, i = 1, 2, \ldots, n.$$

Assumption 2. The activations $f_i(x)$, $g_i(x)$ satisfy the following equation

$$f_i(\pm T_i) = 0, g_i(\pm T_i) = 0, i = 1, 2, \ldots, n.$$

2.2. The definition of fixed-time synchronization

In this subsection, we give the definition of fixed-time synchronization and some lemmas. The error system between the drive system (3) and response system (5) is defined as

$$\begin{cases} \dot{e}_i(t) = \dot{y}_i(t) - \dot{x}_i(t), i = 1, 2, \ldots, n, \\ \dot{e}_i(t) = \dot{\varphi}_i(t) - \dot{\phi}_i(t), t \in [-\tau, 0]. \end{cases} \tag{6}$$

Suppose the origin be a stable point of the error system (5). If the stable point is not origin, we may move to the origin by translation transformation.

Definition 1 [39]**.** The origin of error system (6) is said to be globally uniformly finite-time stable if it is globally uniformly asymptotically stable and there exists a locally bounded function $T : \mathbb{R} \to \mathbb{R}_+ \bigcup\{0\}$, such that $e(t, e_0) = 0$ for all $t \ge T(e_0)$, where $e(\cdot, e_0)$ is an arbitrary solution of the Cauchy problem (6). The function T is called the settling-time function.

Definition 2 [39]**.** The origin of error system (6) is said to be globally fixed-time stable if it is globally uniformly finite-time stable and the settling time T is globally bounded, i.e. $\exists T_{max} \in \mathbb{R}_+$ such that $T(e_0) \le T_{max}, \forall e_0 \in \mathbb{R}^n$.

Remark 3. From the *Definitions 1* and *2*, we can see that the fixed-time stability is an extension of the finite-time stability. And the main difference between the two is whether the settling time T depends on the initial value of the system. The settling time of the finite-time stability depends on the initial value, while the fixed-time stability does not.

According to the definition of the fixed-time stability, we can draw the following definition.

Definition 3. The drive-response systems (1) and (4) are said to achieve fixed-time synchronization if there exists $T(e_0(t))$ in some finite time such that

$$\begin{cases} \lim\limits_{t \to T(e_0(t))} \|e(t)\| = 0, \\ e(t) = 0, \forall t \ge T(e_0(t)) \\ T(e_0(t)) \le T_{max}, \forall e_0(t) \in \mathbb{C}^n[-\tau, 0]. \end{cases} \tag{7}$$

where T_{max} is the settling time, $\|\cdot\|$ represents the Euclidean norm.

Remark 4. According to the *Definition 3*, we transform the problem of fixed-time synchronization between the drive system (1) and response system (4) into the fixed-time stability problem of the error system (6).

Lemma 1 [56]**.** *If there exists a regular, positive definite and radially unbounded function* $V(e(t)): \mathbb{R} \to \mathbb{R}$ *and constants* a, b, δ, $k > 0$ *and* $\delta k > 1$ *meet*

$$\dot{V}(e(t)) \le -\left(aV^{\delta}(e(t)) + b\right)^k, e(t) \in \mathbb{R}^n \backslash 0, \tag{8}$$

then the origin is fixed-time stable, and the settling time T_{max} is estimated by

$$T(e(t_0)) \le T_{max} = \frac{1}{b^k}\left(\frac{b}{a}\right)^{\frac{1}{\delta}}\left(1+\frac{1}{\delta k-1}\right). \tag{9}$$

Lemma 2. *[57] Suppose $x_j(t)$ and $y_j(t)$ are two states of error system (6), then we have*

$$\left|\bigwedge_{j=1}^{n}\alpha_{ij}f_j(x_j(t)) - \bigwedge_{j=1}^{n}\alpha_{ij}f_j(y_j(t))\right| \le \sum_{j=1}^{n}|\alpha_{ij}|\cdot|f_j(x_j(t)) - f_j(y_j(t))|,$$

$$\left|\bigvee_{j=1}^{n}\beta_{ij}f_j(x_j(t)) - \bigvee_{j=1}^{n}\beta_{ij}f_j(y_j(t))\right| \le \sum_{j=1}^{n}|\beta_{ij}|\cdot|f_j(x_j(t)) - f_j(y_j(t))|.$$

Lemma 3. *[58] Let $b_1, b_2, \ldots, b_N \ge 0$, $q>1$, then the following inequality hold*

$$\sum_{i=1}^{N} b_i^q \ge N^{1-q}\left(\sum_{i=1}^{N} b_i\right)^q.$$

Lemma 4. *[59] If Assumptions 1, 2 hold, then we have*

$$\left|K[a_{ij}(y_j(t))]f_j(y_j(t)) - K[a_{ij}(x_j(t))]f_j(x_j(t))\right| \le a_{ij}^m|y_j(t)-x_j(t)|,$$

$$\left|K[b_{ij}(y_j(t))]g_j(y_j(t)) - K[b_{ij}(x_j(t))]g_j(x_j(t))\right| \le b_{ij}^m|y_j(t)-x_j(t)|,$$

i.e. for any $\upsilon_{ij}(x_j(t)) \in K[a_{ij}(x_j(t))]$, $\omega_{ij}(y_j(t)) \in K[a_{ij}(y_j(t))]f_j(y_j(t))$, $i=1,2,\ldots,n$, we also have

$$\left|\omega_{ij}(y_j(t))f_j(y_j(t)) - \upsilon_{ij}(x_j(t))f_j(x_j(t))\right| \le a_{ij}^m|y_j(t)-x_j(t)|,$$

$$\left|\omega_{ij}(y_j(t))g_j(y_j(t)) - \upsilon_{ij}(x_j(t))g_j(x_j(t))\right| \le b_{ij}^m|y_j(t)-x_j(t)|,$$

where $a_{ij}^m = \max\left\{|\tilde{a}_{ij}^{(1)}|, |\tilde{a}_{ij}^{(2)}|\right\}$, $b_{ij}^m = \max\left\{|\tilde{b}_{ij}^{(1)}|, |\tilde{b}_{ij}^{(2)}|\right\}$.

Remark 5. Ref. [56] investigated the fixed-time stability and synchronization of coupled neural networks with discontinuous nonlinear activation functions and without delays, gave a theorem of fixed-time stability and less conservative estimation bound of the settling time. Inspired by this, we borrowed this result to study more complex memristor-based fuzzy cellular neural networks with time-varying delays. In our paper, the design of fixed-time synchronization controllers and the derivation of the results are more complex than Ref. [56].

3. The fixed-time synchronization of the drive-response MFCNN

In this section, we will derive the sufficient conditions of the fixed-time synchronization between the drive system (1) and the response system (4).

In order to obtain these synchronization criteria, we design the fixed-time synchronization controller $u_i(t)$ in the response system (4) as follow

$$\begin{aligned} u_i(t) &= -k_i e_i(t) - sign(e_i(t))\left(\nu_i + \mu_i|e_i(t-\tau_i(t))| + \varrho_i|e_i(t)|^{\iota}\right), \\ & i = 1,2,\ldots,n, \end{aligned} \tag{10}$$

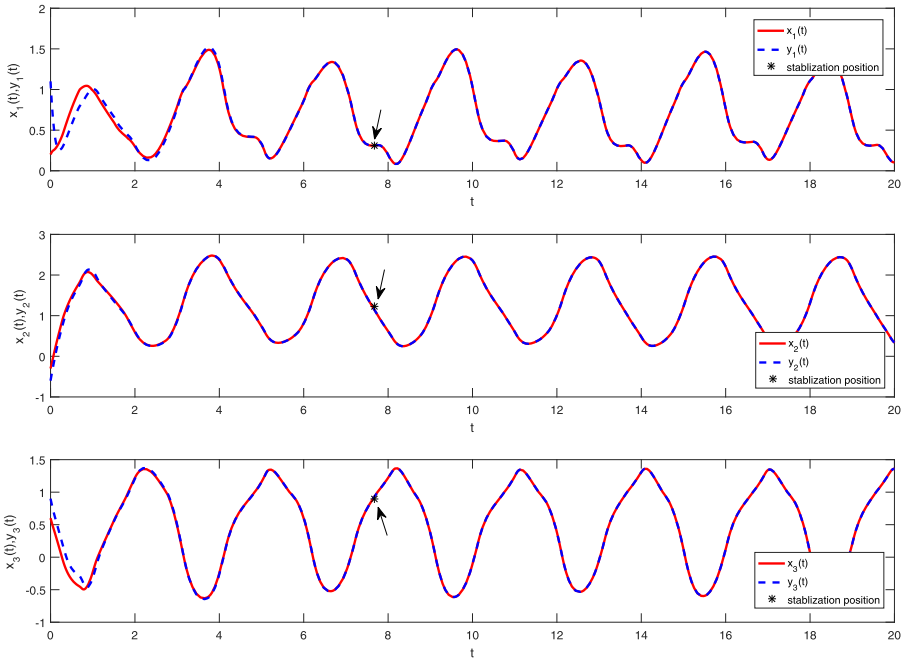

Fig. 5. The trajectories and the stabilization positions of drive-response systems (20) with controller.

where $k_i \geq 0$, $v_i > 0$, $\mu_i > 0$, $\varrho_i > 0$, and $\iota > 1$. $sign(\cdot)$ is the symbolic function.

First, we simplify the error system (6) in order to facilitate the derivation of the main results.

Combined with Eqs. (3), (5) and the controller (10), we calculate the derivative of the error system (6)

$$\begin{aligned}
\dot{e}_i(t) &= \dot{y}_i(t) - \dot{x}_i(t) \\
&= -c_i y_i(t) + \sum_{j=1}^{n} \breve{a}_{ij}(t) f_j(y_j(t)) + \sum_{j=1}^{n} \breve{b}_{ij}(t) g_j(y_j(t-\tau_j(t))) \\
&+ \sum_{j=1}^{n} d_{ij} v_j + \bigwedge_{j=1}^{n} T_{ij} v_j + \bigwedge_{j=1}^{n} \alpha_{ij} g_j(y_j(t-\tau_j(t))) + \bigvee_{j=1}^{n} S_{ij} v_j \\
&+ \bigvee_{j=1}^{n} \beta_{ij} g_j(y_j(t-\tau_j(t))) + I_i + u_i(t) \\
&- \Big(- c_i x_i(t) + \sum_{j=1}^{n} \hat{a}_{ij}(t) f_j(x_j(t)) + \sum_{j=1}^{n} \hat{b}_{ij}(t) g_j(x_j(t-\tau_j(t))) \\
&+ \sum_{j=1}^{n} d_{ij} v_j + \bigwedge_{j=1}^{n} T_{ij} v_j + \bigwedge_{j=1}^{n} \alpha_{ij} g_j(x_j(t-\tau_j(t))) + \bigvee_{j=1}^{n} S_{ij} v_j
\end{aligned}$$

$$
\begin{aligned}
&+\bigvee_{j=1}^{n}\beta_{ij}g_j(x_j(t-\tau_j(t)))+I_i\Big)\\
&=-c_ie_i(t)+\sum_{j=1}^{n}\check{a}_{ij}(t)f_j(y_j(t))-\sum_{j=1}^{n}\hat{a}_{ij}(t)f_j(x_j(t))\\
&+\sum_{j=1}^{n}\check{b}_{ij}(t)g_j(y_j(t-\tau_j(t)))-\sum_{j=1}^{n}\hat{b}_{ij}(t)g_j(x_j(t-\tau_j(t)))\\
&+\bigwedge_{j=1}^{n}\alpha_{ij}g_j(y_j(t-\tau_j(t)))-\bigwedge_{j=1}^{n}\alpha_{ij}g_j(x_j(t-\tau_j(t)))\\
&+\bigvee_{j=1}^{n}\beta_{ij}g_j(y_j(t-\tau_j(t)))-\bigwedge_{j=1}^{n}\alpha_{ij}g_j(x_j(t-\tau_j(t)))\\
&-k_ie_i(t)-\nu_isign(e_i(t))-\mu_isign(e_i(t))|e_i(t-\tau_i(t))|\\
&-\varrho_isign(e_i(t))|e_i(t)|^{\iota}.
\end{aligned}
$$

According to *Assumption 1*, *Lemmas 2* and *4*, we obtain

$$
\begin{aligned}
\dot{e}_i(t)\le&-(c_i+k_i)e_i(t)+\sum_{j=1}^{n}a_{ij}^m|e_i(t)|+\sum_{j=1}^{n}b_{ij}^m|e_i(t-\tau_j(t))|\\
&+\sum_{j=1}^{n}|\alpha_{ij}|\cdot|f_j(y_j(t))-f_j(x_j(t))|+\sum_{j=1}^{n}|\beta_{ij}|\cdot|g_j(y_j(t))-g_j(x_j(t))|\\
&-\nu_isign(e_i(t))-\mu_isign(e_i(t))|e_i(t-\tau_i(t))|-\varrho_isign(e_i(t))|e_j(t)|^{\iota}\\
&\le-(c_i+k_i)e_i(t)+\sum_{j=1}^{n}a_{ij}^m|e_i(t)|+\sum_{j=1}^{n}b_{ij}^m|e_j(t-\tau_j(t))|\\
&+\sum_{j=1}^{n}|\alpha_{ij}|m_j|e_j(t-\tau_j(t))|+\sum_{j=1}^{n}|\beta_{ij}|m_j|e_j(t-\tau_j(t))|\\
&-\nu_isign(e_i(t))-\mu_isign(e_i(t))|e_i(t-\tau_i(t))|-\varrho_isign(e_i(t))|e_i(t)|^{\iota}
\end{aligned}
\tag{11}
$$

Theorem 1. *Under Assumptions 1, 2 and the controller (10), the error system (6) is fixed-time stable if*

$$
\begin{cases}
\displaystyle\sum_{j=1}^{n}a_{ji}^m-c_i-k_i<0,\\
\displaystyle\sum_{j=1}^{n}\left(b_{ji}^m+m_i|\alpha_{ji}|+m_i|\beta_{ji}|\right)-\mu_i<0
\end{cases}
\tag{12}
$$

Furthermore, the settling time can be calculated by the approximate formula

$$
T_s\le T_{max}=\frac{\iota}{\theta(\iota-1)}\left(\frac{\theta}{\lambda n^{1-\iota}}\right)^{\frac{1}{\iota}}.
\tag{13}
$$

where $\lambda=\min_{1\le i\le n}\{\varrho_i\}$, $\theta=\sum_{i=1}^{n}\nu_i$.

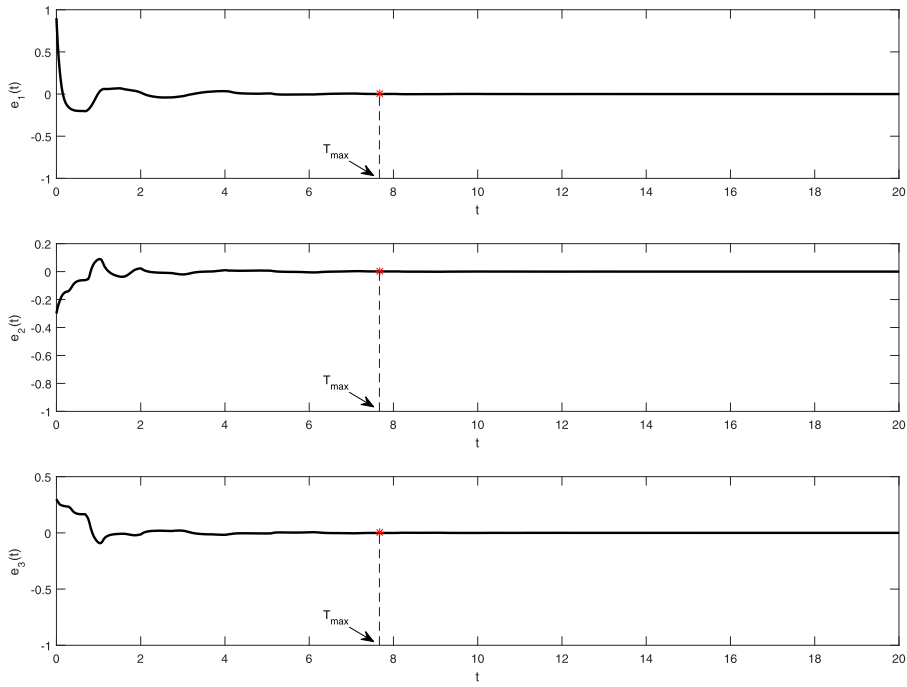

Fig. 6. The error curves and the settling time (T_{max}) of drive-response systems (20) with the controller.

Proof. Consider a Lyapunov function defined by

$$V(e(t)) = \sum_{i=1}^{n} |e_i(t)|. \tag{14}$$

Obviously, $V(e(t)) \geq 0$ and $V(e(t)) = 0$ if and only if $e(t) = 0$. $V(e(t))$ is regular, positive definite and radially unbounded. Next, we discuss $e_i(t) = 0$ and $e_i(t) \neq 0$ $(i = 1, 2, \ldots, n)$, respectively.

(1) When $e_i(t) = 0$, the error system (6) is in steady state at time t. According to the controller (10), we know that $u_i(t) = 0$ at this time. Therefore, we can always find suitable controller parameters to meet conditions (12) and (13).

(2) When $e_i(t) \neq 0$, we have $sign(e_i(t)) \times sign(e_i(t)) = 1$. Calculating the upper right-hand derivative of Eq. (14) along the error system (6) and replacing the $\dot{e}_i(t)$ with the inequality (11), we have

$$\begin{aligned}
\dot{V}(e(t)) &= \sum_{i=1}^{n} sign(e_i(t))\dot{e}_i(t) \\
&\leq \sum_{i=1}^{n} sign(e_i(t))\Big(-(c_i + k_i)e_i(t) + \sum_{j=1}^{n} a_{ij}^{m}|e_i(t)| + \sum_{j=1}^{n} b_{ij}^{m}|e_j(t - \tau_j(t))| \\
&+ \sum_{j=1}^{n} |\alpha_{ij}|m_j|e_j(t - \tau_j(t))| + \sum_{j=1}^{n} |\beta_{ij}|m_j|e_j(t - \tau_j(t))|
\end{aligned}$$

$$
\begin{aligned}
&-\nu_i sign(e_i(t)) - \mu_i sign(e_i(t))|e_i(t-\tau_i(t))| - \varrho_i sign(e_i(t))|e_i(t)|^{\iota}\Big) \\
&\le \sum_{i=1}^{n}\Big(-(c_i+k_i)|e_i(t)|\Big) + \sum_{i=1}^{n}\sum_{j=1}^{n} a_{ij}^{m}|e_j(t)| + \sum_{i=1}^{n}\sum_{j=1}^{n} b_{ij}^{m}|e_j(t-\tau_j(t))| \\
&+ \sum_{i=1}^{n}\sum_{j=1}^{n}|\alpha_{ij}|m_j|e_j(t-\tau_j(t))| + \sum_{i=1}^{n}\sum_{j=1}^{n}|\beta_{ij}|m_j|e_j(t-\tau_j(t))| \\
&- \sum_{i=1}^{n}\nu_i - \sum_{i=1}^{n}\mu_i|e_i(t-\tau_i(t))| - \sum_{i=1}^{n}\varrho_i|e_i(t)|^{\iota} \\
&= \sum_{i=1}^{n}\Big(\sum_{j=1}^{n} a_{ji}^{m} - c_i - k_i\Big)|e_i(t)| \\
&+ \sum_{i=1}^{n}\Big(\sum_{j=1}^{n}(b_{ji}^{m} + m_i|\alpha_{ji}| + m_i|\beta_{ji}|) - \mu_i\Big)|e_i(t-\tau_i(t))| \\
&- \sum_{i=1}^{n}\nu_i - \sum_{i=1}^{n}\varrho_i|e_i(t)|^{\iota}.
\end{aligned}
$$

When choosing the appropriate controller parameters to meet the condition (12), we have the following inequalities

$$\dot{V}(e(t)) \le -\sum_{i=1}^{n}\varrho_i|e_i(t)|^{\iota} - \sum_{i=1}^{n}\nu_i$$

Let $\lambda = \min_{1\le i\le n}\{\varrho_i\}, \theta = \sum_{i=1}^{n}\nu_i$, and by *Lemma 3*, we obtain

$$\dot{V}(e(t)) \le -\lambda n^{1-\iota}(V(e(t)))^{\iota} - \theta$$

Let $k = 1$ in *Lemma 1*, we know the origin is fixed-time stable, and the settling time T_{max}

$$T_s \le T_{max} = \frac{\iota}{\theta(\iota-1)}\left(\frac{\theta}{\lambda n^{1-\iota}}\right)^{\frac{1}{\iota}}.$$

This proof is finished. □

Immediately, we have the following corollary based the equivalence between the stability of error system (6) and the synchronization of the drive-response systems (1) and (4).

Corollary 1. *The drive system (1) and the response system (4) can be achieved to fixed-time synchronization when the conditions (12) hold, and the settling time T_{max} can be given by Eq. (13).*

Remark 6. Due to the use of improved *Lemma 1*, compared with the previous fixed-time synchronization of neural network [40,60,61], the controller is greatly simplified.

Remark 7. According to Eq. (13), we know that the settling time T_s is related to the ν_i, ϱ_i and ι in the controller (10). Under the condition of satisfying the theorem, the value of the

settling time can be changed by modifying the values of these parameters. This is conducive to the real system according to different circumstances to choose the appropriate settling time.

Remark 8. From the conditions (11) and the approximate formula (12), we can know the roles of each term in control input $u_i(t)$. In controller (19), k_i, μ_i and all parameters of the error system together constitute the sufficient conditions of fixed-time stability. ν_i and ϱ_i determine the settling time T_{max} of the error system.

If there are not the elements of delay feedback template, fuzzy feedback MIN template and fuzzy feedback MAX template in the system (1), i.e. $\tilde{b}_{ij}(x_j(t-\tau_j(t))) = \alpha_{ij} = \beta_{ij} = 0$, then the corresponding drive-response system is changed to the following form

$$\begin{cases} \dot{x}_i(t) = -c_i x_i(t) + \sum_{j=1}^{n} \hat{a}_{ij}(t) f_j(x_j(t)) + \sum_{j=1}^{n} d_{ij} v_j + \bigwedge_{j=1}^{n} T_{ij} v_j + \bigvee_{j=1}^{n} S_{ij} v_j + I_i. \\ \dot{y}_i(t) = -c_i y_i(t) + \sum_{j=1}^{n} \check{a}_{ij}(t) f_j(y_j(t)) + \sum_{j=1}^{n} d_{ij} v_j + \bigwedge_{j=1}^{n} T_{ij} v_j + \bigvee_{j=1}^{n} S_{ij} v_j + I_i \\ \qquad + u_i(t), i = 1, 2, \ldots, n. \end{cases} \tag{15}$$

Here, the fixed-time synchronization controller (10) can also be reduced to the following form

$$u_i(t) = -k_i e_i(t) - sign(e_i(t))(\nu_i + \varrho_i |e_i(t)|^{\iota}), i = 1, 2, \ldots, n. \tag{16}$$

Corollary 2. *Under Assumptions 1, 2 and the controller (16), the drive-response system (15) can achieve fixed-time synchronization if*

$$\sum_{j=1}^{n} a_{ji}^{m} - c_i - k_i < 0, i = 1, 2, \ldots, n. \tag{17}$$

Moreover, the settling-time T_s can be obtained from Eq. (13).

Proof. The proof process is similar to *Theorem 1* and is omitted here.

The results of *Theorem 1* can also easily extend to the general memristor-based cellular neural network which does not contain fuzzy items. Considering the following drive-response systems

$$\begin{cases} \dot{x}_i(t) = -c_i x_i(t) + \sum_{j=1}^{n} \hat{a}_{ij}(t) f_j(x_j(t)) + \sum_{j=1}^{n} \hat{b}_{ij}(t) g_j(x_j(t-\tau_j(t))) + I_i, \\ x_i(t) = \phi_i(t), t \in [-\tau, 0], i = 1, 2, \ldots, n, \\ \dot{y}_i(t) = -c_i y_i(t) + \sum_{j=1}^{n} \check{a}_{ij}(t) f_j(y_j(t)) + \sum_{j=1}^{n} \check{b}_{ij}(t) g_j(y_j(t-\tau_j(t))) + I_i + u_i(t). \\ y_i(t) = \varphi_i(t), t \in [-\tau, 0], i = 1, 2, \ldots, n, \end{cases} \tag{18}$$

For the drive-response system (18), we have the following corollary. □

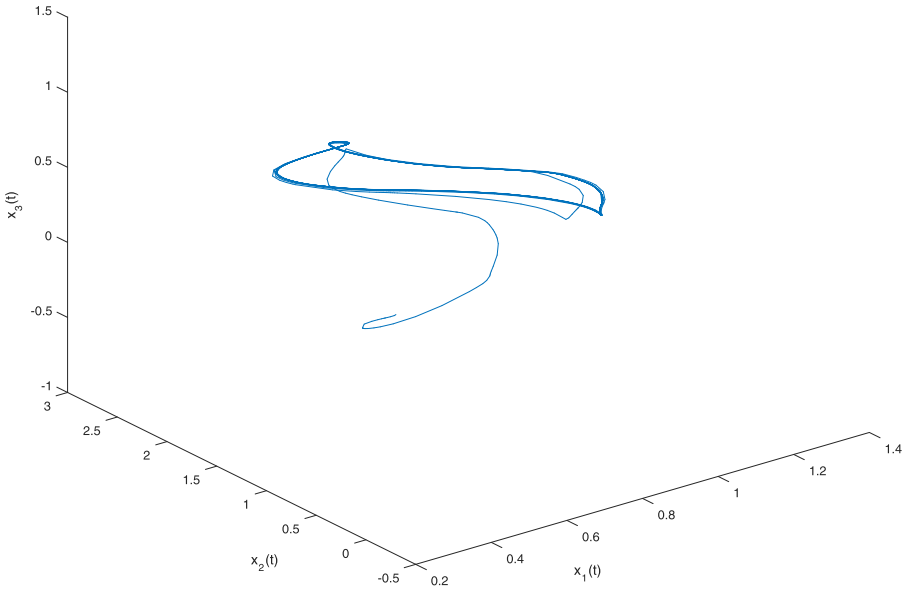

Fig. 7. The phase diagram of FCNN.

Corollary 3. *Under Assumptions 1, 2 and the controller (10), the drive-response system can achieve fixed-time synchronization if*

$$\begin{cases} \sum_{j=1}^{n} a_{ji}^{m} - c_i - k_i < 0, \\ \sum_{j=1}^{n} b_{ji}^{m} - \mu_i < 0. \end{cases} \tag{19}$$

Moreover, the settling-time T_s can be obtained from Eq. (13).

Proof. The proof process is similar to *Theorem 1* and is omitted here. □

Remark 9. There have been some literatures to study the fixed-time synchronization problems of general neural networks with memristor or without memristor [41,42,56,60,61]. Compared with previous studies, the conditions of *Theorem 3* are easier to be verified, and the synchronization controller (10) is simpler.

4. Numerical examples

In this section, we give three numerical examples in order to verify the effectiveness of the theoretical results of Theorem 1, **Corollaries 2** and **3**.

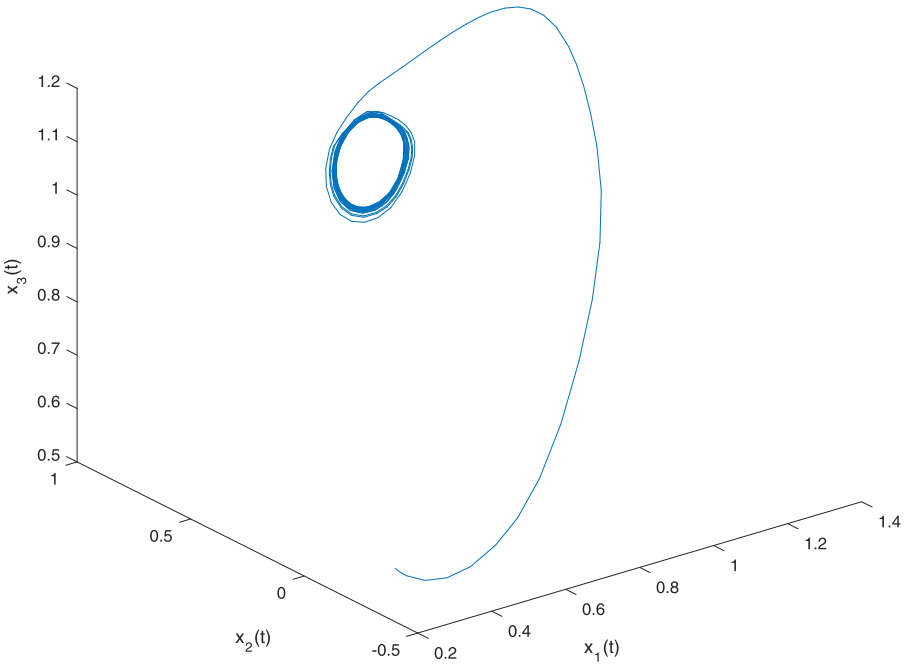

Fig. 8. The phase diagram of the drive system in Eq. (21) when the initial value $\phi(t)$=[0.2;-0.4;0.6].

Example 1 Consider the following three-dimensional drive-response memristor-based fuzzy cellular neural network

$$
\begin{cases}
\dot{x}_i(t) = -c_i x_i(t) + \sum_{j=1}^{3} \tilde{a}_{ij}(x_j(t)) f_j(x_j(t)) + \sum_{j=1}^{3} \tilde{b}_{ij}(x_j(t-\tau_j(t))) g_j(x_j(t-\tau_j(t))) \\
\quad + \sum_{j=1}^{3} d_{ij} v_j + \bigwedge_{j=1}^{3} T_{ij} v_j + \bigwedge_{j=1}^{3} \alpha_{ij} g_j(x_j(t-\tau_j(t))) + \bigvee_{j=1}^{3} S_{ij} v_j \\
\quad + \bigvee_{j=1}^{3} \beta_{ij} g_j(x_j(t-\tau_j(t))) + I_i, \\
\dot{y}_i(t) = -c_i y_i(t) + \sum_{j=1}^{3} \tilde{a}_{ij}(y_j(t)) f_j(y_j(t)) + \sum_{j=1}^{3} \tilde{b}_{ij}(y_j(t-\tau_j)) g_j(y_j(t-\tau_j(t))) \\
\quad + \sum_{j=1}^{3} d_{ij} v_j + \bigwedge_{j=1}^{3} T_{ij} v_j + \bigwedge_{j=1}^{3} \alpha_{ij} g_j(y_j(t-\tau_j(t))) + \bigvee_{j=1}^{3} S_{ij} v_j \\
\quad + \bigvee_{j=1}^{3} \beta_{ij} g_j(y_j(t-\tau_j(t))) + I_i + u_i(t), i = 1, 2, 3,
\end{cases}
\tag{20}
$$

The parameters of Eq. (20) are listed below

$$\tilde{a}_{11}(x_1)=\begin{cases}-0.8, |x_1|\le 1\\ -1, |x_1|>1\end{cases}\tilde{a}_{12}(x_1)=\begin{cases}2.2, |x_1|\le 1\\ 2, |x_1|>1\end{cases}\tilde{a}_{13}(x_1)=\begin{cases}1.2, |x_1|\le 1\\ 1.8, |x_1|>1\end{cases}$$

$$\tilde{a}_{21}(x_2)=\begin{cases}1, |x_2|\le 1\\ 0.8, |x_2|>1\end{cases}\tilde{a}_{22}(x_2)=\begin{cases}-1, |x_2|\le 1\\ -0.8, |x_2|>1\end{cases}\tilde{a}_{23}(x_2)=\begin{cases}-2.4, |x_2|\le 1\\ -2, |x_2|>1\end{cases}$$

$$\tilde{a}_{31}(x_3)=\begin{cases}0.2, |x_3|\le 1\\ 0.4, |x_3|>1\end{cases}\quad\tilde{a}_{32}(x_3)=\begin{cases}-0.6, |x_3|\le 1\\ -0.4, |x_3|>1\end{cases}\tilde{a}_{33}(x_3)=\begin{cases}1.8, |x_3|\le 1\\ 1.2, |x_3|>1\end{cases}$$

$$\tilde{b}_{11}(x_1)=\begin{cases}-3.2, |x_1|\le 1\\ -3, |x_1|>1\end{cases}\tilde{b}_{12}(x_1)=\begin{cases}0.2, |x_1|\le 1\\ 0.4, |x_1|>1\end{cases}\tilde{b}_{13}(x_1)=\begin{cases}1, |x_1|\le 1\\ 1.5, |x_1|>1\end{cases}$$

$$\tilde{b}_{21}(x_2)=\begin{cases}0.4, |x_2|\le 1\\ 0.2, |x_2|>1\end{cases}\quad\tilde{b}_{22}(x_2)=\begin{cases}-3.6, |x_2|\le 1\\ -3.2, |x_2|>1.\end{cases}\tilde{b}_{23}(x_2)=\begin{cases}1.5, |x_2|\le 1\\ 2.1, |x_2|>1.\end{cases}$$

$$\tilde{b}_{31}(x_3)=\begin{cases}2.2, |x_3|\le 1\\ 2.6, |x_3|>1\end{cases}\tilde{b}_{32}(x_3)=\begin{cases}3.2, |x_3|\le 1\\ 2.8, |x_3|>1\end{cases}\quad\tilde{b}_{33}(x_3)=\begin{cases}-2.6, |x_3|\le 1\\ -2.4, |x_3|>1\end{cases}$$

Note: In order to simplify the expression, $\tilde{a}_{ij}(x_j)$ and the following $|x_j|$ denote $\tilde{a}_{ij}(x_j(t))$ and $|x_j(t)|$, $\tilde{b}_{ij}(x_j)$ and the following $|x_j|$ denote $\tilde{b}_{ij}(x_j(t-\tau_j(t)))$ and $|x_j(t-\tau_j(t))|$, respectively.

$c=[1;\ 1.5;\ 2]$; $f_i(x)=g_i(x)=0.5\big||x+1|-|x-1|\big|-1$;

$$A=\begin{bmatrix}-0.1 & -0.01 & 0.2\\ -0.2 & -0.1 & 0.1\\ -0.04 & -0.2 & 0.4\end{bmatrix};\ B=\begin{bmatrix}-0.1 & -0.01 & 0.3\\ -0.1 & -0.2 & 0.2\\ -0.1 & -0.2 & 0.3\end{bmatrix};\ D=\begin{bmatrix}0.5 & 0.1 & -0.4\\ 0.1 & 0.5 & -0.2\\ 0.2 & 0.4 & 0.5\end{bmatrix};$$

$$T=\begin{bmatrix}0.2 & 0.1 & 0.4\\ 0.2 & 0.2 & 0.6\\ 0.5 & 0.3 & 0.2\end{bmatrix};\ S=\begin{bmatrix}0.2 & 0.1 & 0.2\\ 0.2 & 0.2 & 0.4\\ 0.8 & 0.1 & 0.2\end{bmatrix};\ V=[1;\ 2;\ 1];$$

$\tau_i(t)=e^t/(1+e^t)$; $\phi_1(t)=0.2+0.1sin(t)$; $\phi_2(t)=-0.4+0.1cos(t)$; $\phi_3(t)=0.6+0.1sin(t)$;
$\varphi_1(t)=1.2-0.1sin(t)$; $\varphi_2(t)=-0.6-0.1cos(t)$; $\varphi_3(t)=1-0.1sin(t)$; $I=[0;\ 0;\ 0]$,

where $A=(\alpha_{ij})_{3\times 3}, B=(\beta_{ij})_{3\times 3}, D=(d_{ij})_{3\times 3}, T=(T_{ij})_{3\times 3}, S=(S_{ij})_{3\times 3}, V=[v1;\ v2;\ v3]$, $i,\ j=1,2,3$.

Figs. (2) and (3) show the phase diagram and trajectories of the drive system in (20) when there is no controller. Fig. (2) illustrates that the current parameters makes the drive system in Eq. (20) have a limit cycle. Fig. (3) indicates that the drive system and the response do not reach synchronization state.

Firstly, we will verify the condition of Theorem 1. In controller (10), let $k=[2;\ 3;\ 4]$, $\nu=[1;\ 1;\ 1]$, $\mu=[8;\ 8;\ 8]$, $\varrho=[1;\ 1;\ 1]$, $\iota=1.5>1$. Thus, the controller $u_i(t)$ can be represented

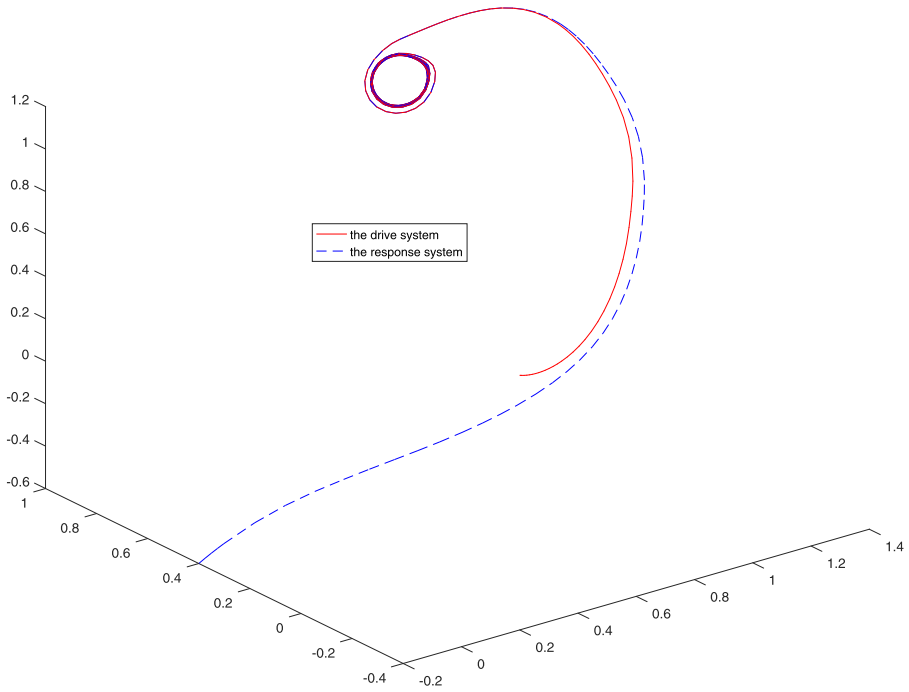

Fig. 9. The phase diagram of the drive-response system (21) with controller.

as follows.

$$\begin{cases} u_1(t) = -2e_1(t) - sign(e_1(t))\left(1 + 8|e_1\left(t - \dfrac{e^t}{1+e^t}\right)| + |e_1(t)|^{1.5}\right), \\ u_2(t) = -3e_2(t) - sign(e_2(t))\left(1 + 8|e_2\left(t - \dfrac{e^t}{1+e^t}\right)| + |e_2(t)|^{1.5}\right), \\ u_3(t) = -4e_3(t) - sign(e_3(t))\left(1 + 8|e_3\left(t - \dfrac{e^t}{1+e^t}\right)| + |e_3(t)|^{1.5}\right), \end{cases}$$

Let Lipschitz constant $m = [0.5; 0.5; 0.5]$. From the parameters of the system (20), we have $A^m = (a_{ij}^m)_{3\times 3} = \begin{bmatrix} 1 & 2.2 & 1.8 \\ 1 & 1 & 2.4 \\ 0.4 & 0.6 & 1.8 \end{bmatrix}$, $B^m = (b_{ij}^m)_{3\times 3} = \begin{bmatrix} 3.2 & 0.4 & 1.5 \\ 0.4 & 3.6 & 2.1 \\ 2.6 & 3.2 & 2.6 \end{bmatrix}$. Through simple calculations, we get

$$\sum_{j=1}^{3} a_{j1}^m - c_1 - k_1 = -0.6 < 0,$$

$$\sum_{j=1}^{3} a_{j2}^m - c_2 - k_2 = -0.7 < 0,$$

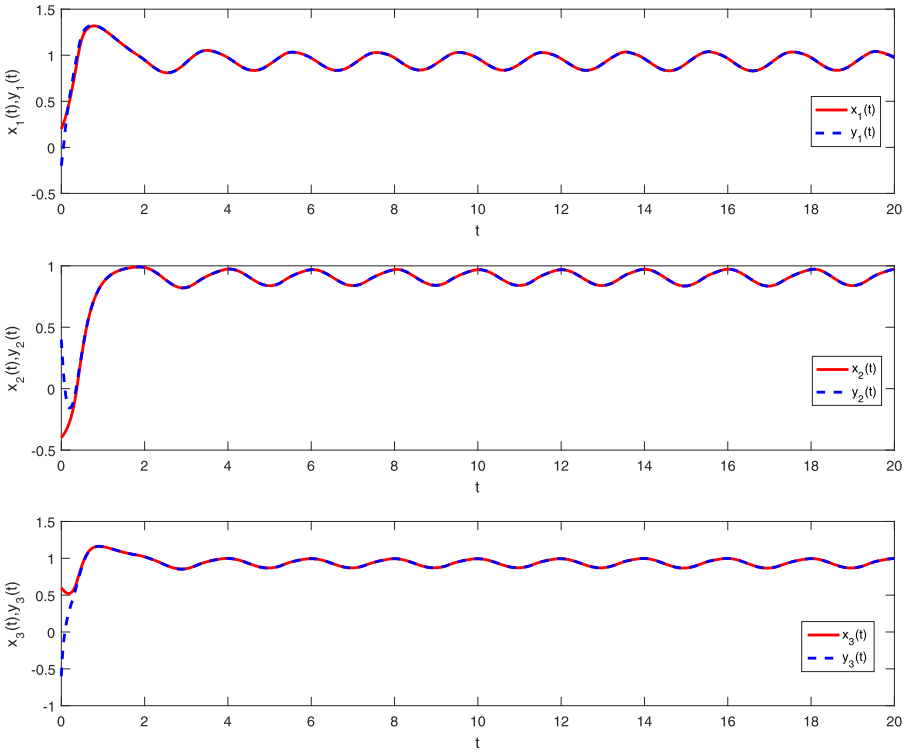

Fig. 10. The trajectories of drive-response system (21) with the controller.

$$\sum_{j=1}^{3} a_{j3}^{m} - c_3 - k_3 = -0.5 < 0,$$

$$\sum_{j=1}^{3} \left(b_{j1}^{m} + m_1|\alpha_{j1}| + m_1|\beta_{j1}|\right) - \mu_1 = -1.48 < 0,$$

$$\sum_{j=1}^{3} \left(b_{j2}^{m} + m_2|\alpha_{j2}| + m_2|\beta_{j2}|\right) - \mu_2 = -0.44 < 0,$$

$$\sum_{j=1}^{3} \left(b_{j3}^{m} + m_3|\alpha_{j3}| + m_3|\beta_{j3}|\right) - \mu_3 = -1.05 < 0.$$

The conditions of *Theorem 1* are satisfied. Figs. (4) and (5) illustrate the phase diagram, trajectories of the drive-response system (20), respectively.

Fig. (6) shows the error curves of of the drive-response system (20).

Fig. (4) shows that under the controller (10), the drive and response systems (20) with different initial points eventually have the same limit cycle as Fig. (2). Compared with Fig. (3), it can be seen from Fig. (5) that the state trajectory curves of (20) reach synchronization within a fixed time T_{max}. The error system curves Fig. (6) validate this again.

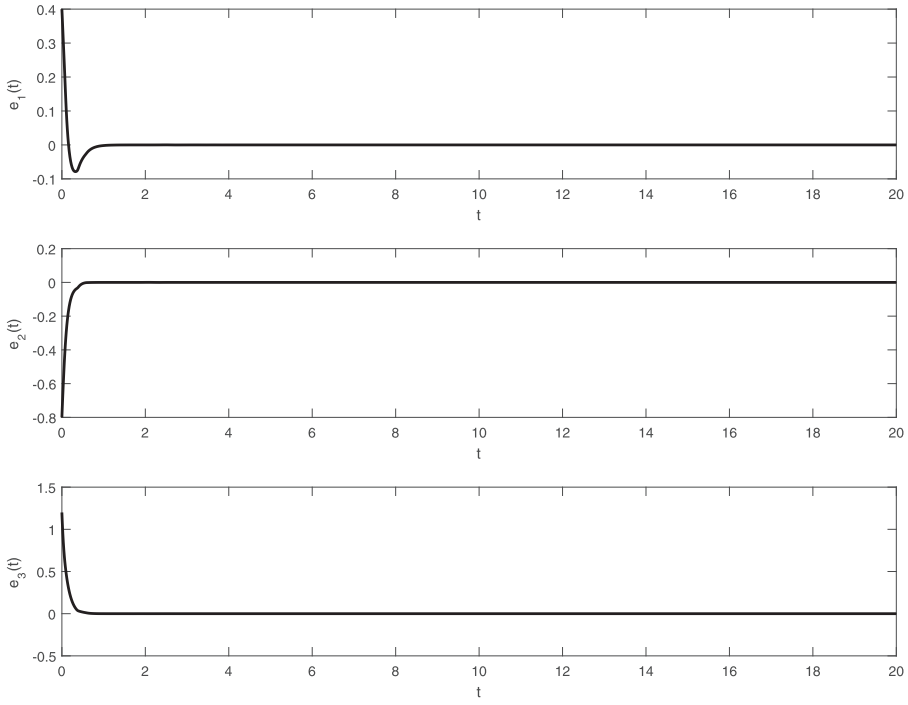

Fig. 11. The error curves of drive-response system (21) with the controller.

Secondly, we calculate the settling time T_{max} by Eq. (13). Using the parameters of the controller (10), we have $\lambda = 1, \theta = 3, \iota = 1.15$. Thus, the settling time $T_{max} = 7.667$. From Fig. (6), we can see that the synchronization is achieved within T_{max}.

Remark 10. In *Example 1*, we also did the simulation of the MFCNN without memristors, i.e. the weight values $\tilde{a}_{ij}, \tilde{b}_{ij}$ are fixed. The simulation results show that except for the phase diagram or trajectories of the model, as show in Fig. 7, the method proposed in this paper can also make the drive-response FCNNs achieve the fixed-time synchronization.

Example 2. Consider the following three-dimensional drive-response memristor-based fuzzy cellular neural network without delay items.

$$\begin{cases} \dot{x}_i(t) = -c_i x_i(t) + \sum_{j=1}^{3} \tilde{a}_{ij}(x_j(t)) f_j(x_j(t)) + \sum_{j=1}^{3} d_{ij} v_j + \bigwedge_{j=1}^{3} T_{ij} v_j + \bigvee_{j=1}^{3} S_{ij} v_j + I_i. \\ \dot{y}_i(t) = -c_i y_i(t) + \sum_{j=1}^{3} \tilde{a}_{ij}(y_j(t)) f_j(y_j(t)) + \sum_{j=1}^{3} d_{ij} v_j + \bigwedge_{j=1}^{3} T_{ij} v_j + \bigvee_{j=1}^{3} S_{ij} v_j + I_i \\ \qquad + u_i(t), i = 1, 2, 3. \end{cases} \tag{21}$$

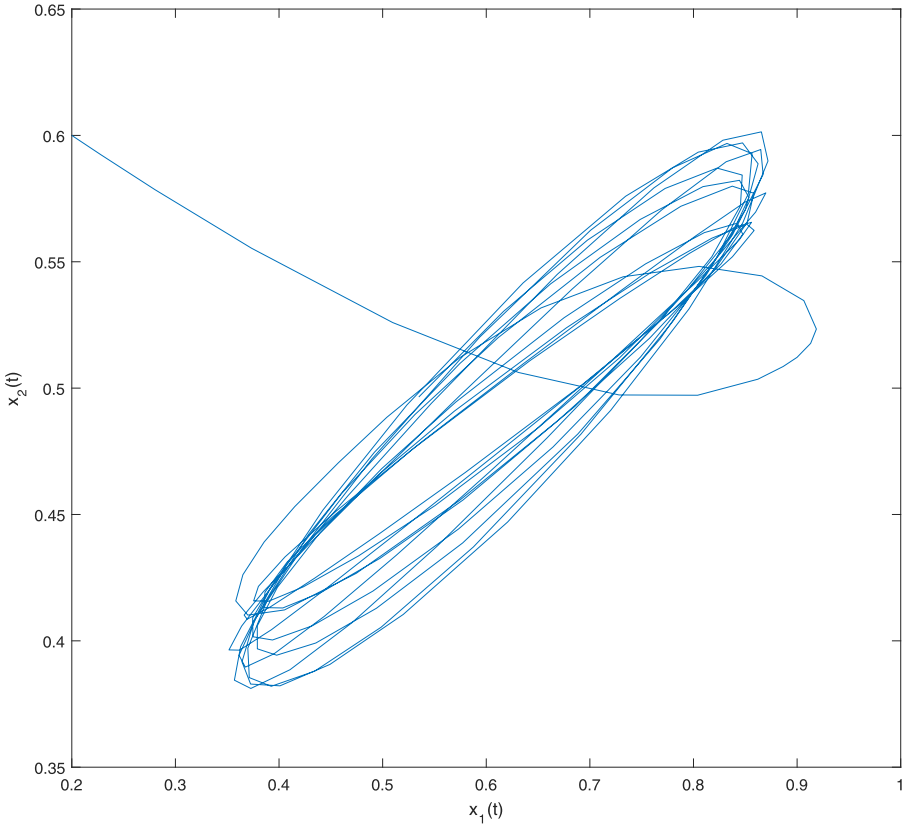

Fig. 12. The phase diagram of the drive system in Eq. (22) without the controller (10) when the initial value $\phi(0)$=[0.2;0.6].

The weight parameters of Eq. (21) are listed below

$$\tilde{a}_{11}(x_1)=\begin{cases}2.5, |x_1|\le 1\\ 2.6, |x_1|>1\end{cases}\quad \tilde{a}_{12}(x_2)=\begin{cases}-2.0, |x_2|\le 1\\ -2.2, |x_2|>1\end{cases}\quad \tilde{a}_{13}(x_3)=\begin{cases}-3.0, |x_3|\le 1\\ -3.4, |x_3|>1\end{cases}$$

$$\tilde{a}_{21}(x_1)=\begin{cases}2.2, |x_1|\le 1\\ 2.6, |x_1|>1\end{cases}\quad \tilde{a}_{22}(x_2)=\begin{cases}-1.8, |x_2|\le 1\\ -2.2, |x_2|>1\end{cases}\quad \tilde{a}_{23}(x_3)=\begin{cases}2.4, |x_3|\le 1\\ 2.2, |x_3|>1\end{cases}$$

$$\tilde{a}_{31}(x_1)=\begin{cases}2.2, |x_1|\le 1\\ 2.8, |x_1|>1\end{cases}\quad \tilde{a}_{32}(x_2)=\begin{cases}-2.4, |x_2|\le 1\\ -2.2, |x_2|>1\end{cases}\quad \tilde{a}_{33}(x_x)=\begin{cases}3.6, |x_3|\le 1\\ 3.2, |x_3|>1\end{cases}$$

The parameters c_i, d_{ij}, S_{ij}, T_{ij}, I_i are the same as *Example 1*. The initial values of Eq. (21) are $\phi(t)=[0.2;-0.4;0.6]$, and $\varphi(t)=[-0.2;0.4;-0.6]$, respectively. Fig. (8) shows the phase diagram of the drive system in Eq. (21).

Similarly, we will verify the conditions of Corollary 2. Let $k=[4.3;5.0;6.8]$, $\nu=[1;1;1]$, $\varrho=[1;1;1]$. From the parameters of Eq. (21), we have $A^m=(a_{ij}^m)_{3\times 3}=$

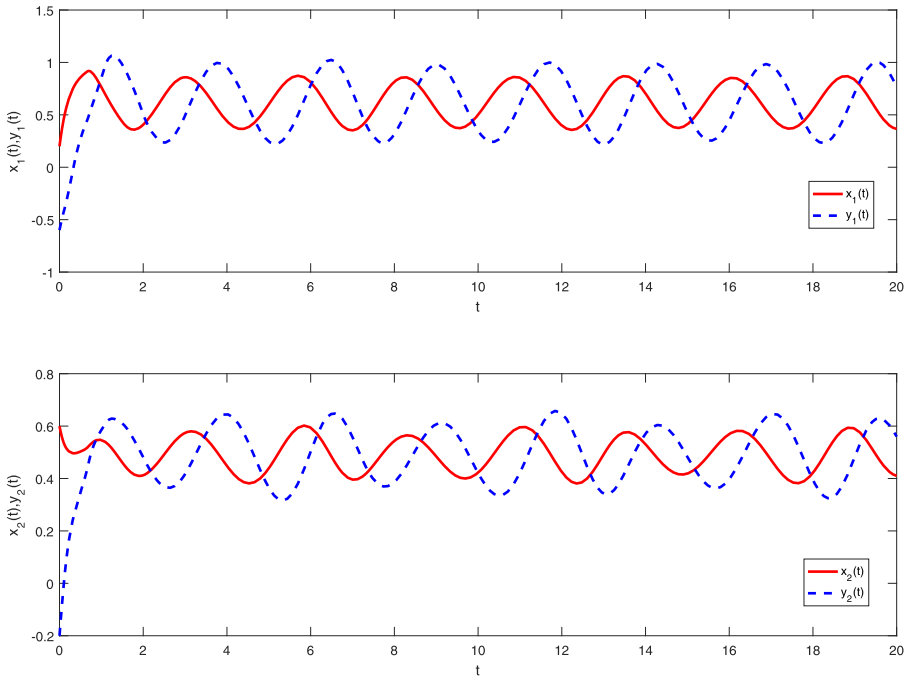

Fig. 13. The trajectories of drive-response system (22) without the controller.

$\begin{bmatrix} 1.6 & 0.2 & 1.4 \\ 1.6 & 2.2 & 1.4 \\ 1.8 & 2.4 & 2.4 \end{bmatrix}$. According to the conditions (17), we get

$$\sum_{j=1}^{3} a_{j1}^{m} - c_1 - k_1 = -0.5 < 0,$$

$$\sum_{j=1}^{3} a_{j2}^{m} - c_2 - k_2 = -0.2 < 0,$$

$$\sum_{j=1}^{3} a_{j3}^{m} - c_3 - k_3 = -0.5 < 0.$$

Obviously, The conditions of Corollary 2 are satisfied. Fig.s (9) and (10) illustrate the phase diagram, trajectories of the drive-response system (21), respectively.

Fig. (11) shows the error curves of of the drive-response system (21).

Similarly, we calculate the settling time T_{max} by Eq. (13). Using the parameters of the controller (16), we have $\lambda = 1, \theta = 3, \iota = 1.5$. Thus, the settling time $T_{max} = 3.0$. The settling time in *Example 1* is the same as that in *Example 2*, which verifies the correctness of Corollary 2.

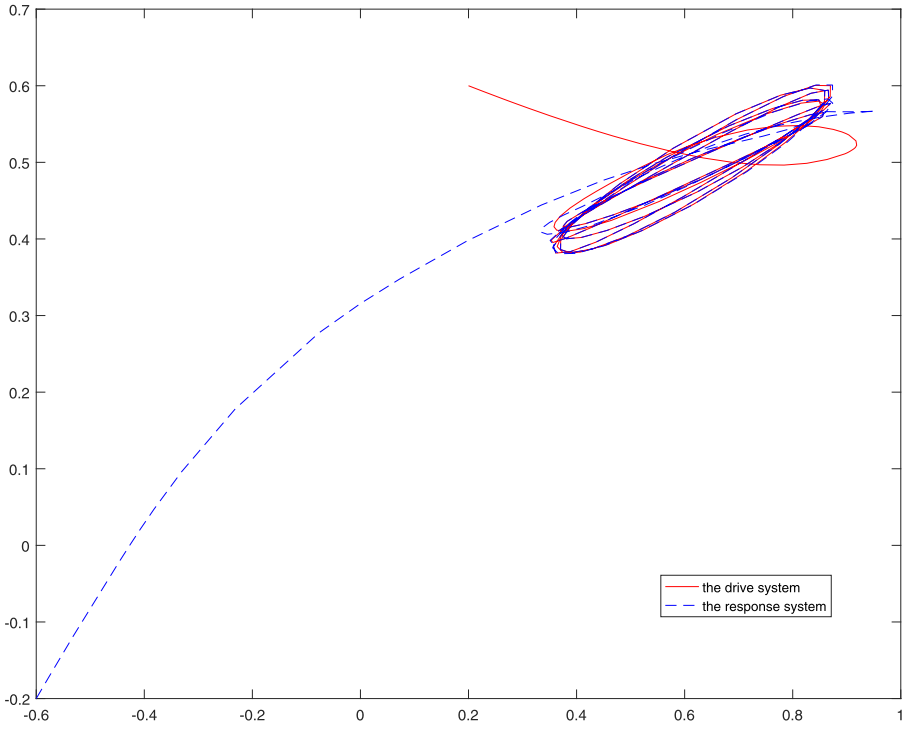

Fig. 14. The phase diagram of the drive-response system (22) with controller.

Example 3 Consider the following two-dimensional memristor-based cellular neural network without fuzzy items.

$$\begin{cases} \dot{x}_i(t) = -c_i x_i(t) + \sum_{j=1}^{2} \tilde{a}_{ij}(x_j(t)) f_j(x_j(t)) + \sum_{j=1}^{2} \tilde{b}_{ij}(x_j(t-\tau_j(t))) g_j(x_j(t-\tau_j(t))) + I_i, \\ \dot{y}_i(t) = -c_i y_i(t) + \sum_{j=1}^{2} \tilde{a}_{ij}(y_j(t)) f_j(y_j(t)) + \sum_{j=1}^{2} \tilde{b}_{ij}(y_j(t-\tau_j)) g_j(y_j(t-\tau_j(t))) + I_i \\ \qquad + u_i(t), i = 1, 2. \end{cases} \tag{22}$$

The corresponding weight parameters are as follows

$$\tilde{a}_{11}(x_1) = \begin{cases} -1.8, |x_1| \le 1 \\ -1.5, |x_1| > 1 \end{cases} \quad \tilde{a}_{12}(x_1) = \begin{cases} 2.8, |x_1| \le 1 \\ 2.5, |x_1| > 1 \end{cases}$$

$$\tilde{a}_{21}(x_2) = \begin{cases} 1, |x_2| \le 1 \\ 0.8, |x_2| > 1 \end{cases} \quad \tilde{a}_{22}(x_2) = \begin{cases} -1, |x_2| \le 1 \\ -0.8, |x_2| > 1. \end{cases}$$

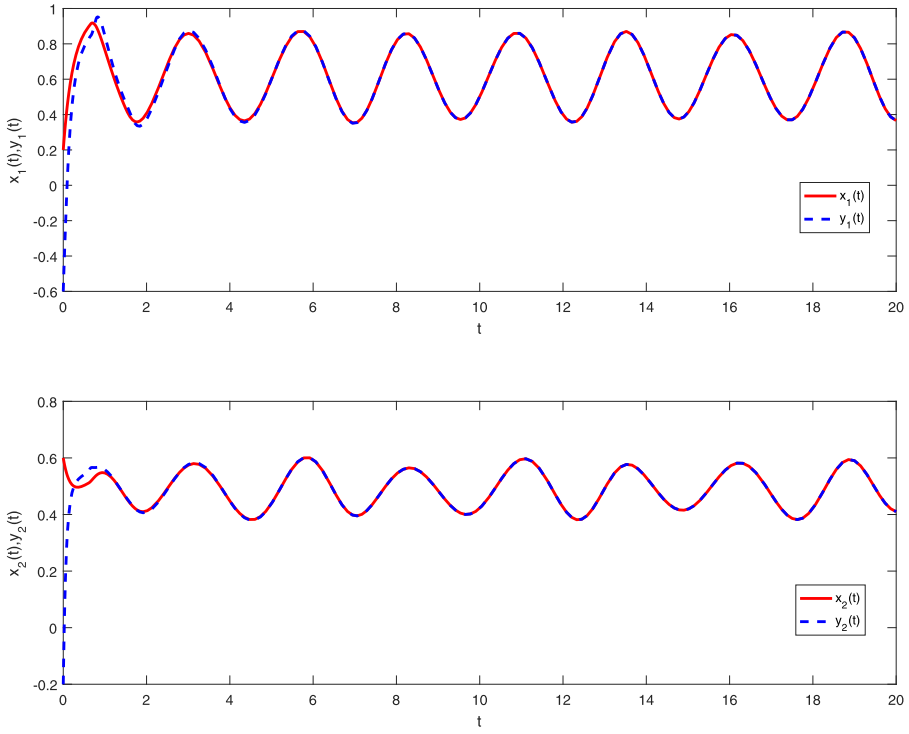

Fig. 15. The trajectories of drive-response system (22) with the controller.

$$\tilde{b}_{11}(x_1) = \begin{cases} -3.5, |x_1| \le 1 \\ -3.2, |x_1| > 1. \end{cases} \quad \tilde{b}_{12}(x_1) = \begin{cases} -1.2, |x_1| \le 1 \\ -1.5, |x_1| > 1 \end{cases}$$

$$\tilde{b}_{21}(x_1) = \begin{cases} -0.1, |x_2| \le 1 \\ -0.2, |x_2| > 1 \end{cases} \quad \tilde{b}_{22}(x_2) = \begin{cases} -1.6, |x_2| \le 1 \\ -1.2, |x_2| > 1 \end{cases}$$

$c = [2; 2], I = [0; 0], \phi(t) = [0.2; 0.6]; \varphi(t) = [-0.6; -0.2].$

Under the above parameters, the phase diagram of the drive system In Eq. (22) is shown in Fig. (12) when no controller. Fig. (13) shows the trajectories of the drive-response system (22).

In controller (10), let $k = [2; 4], \nu = [1; 1], \mu = [6; 6], \varrho = [1; 1], \iota = 1.2$. According to the parameters of drive-response system (22), we get $A^m = \begin{bmatrix} 1.8 & 2.8 \\ 1 & 1 \end{bmatrix}$, $B^m = \begin{bmatrix} 3.5 & 1.5 \\ 0.2 & 1.6 \end{bmatrix}$. Thus, the conditions of *Theorem 3* is calculated as follows

$$\sum_{j=1}^{2} a_{j1}^m - c_1 - k_1 = -1.2 < 0,$$

$$\sum_{j=1}^{2} a_{j2}^m - c_2 - k_2 = -2.2 < 0,$$

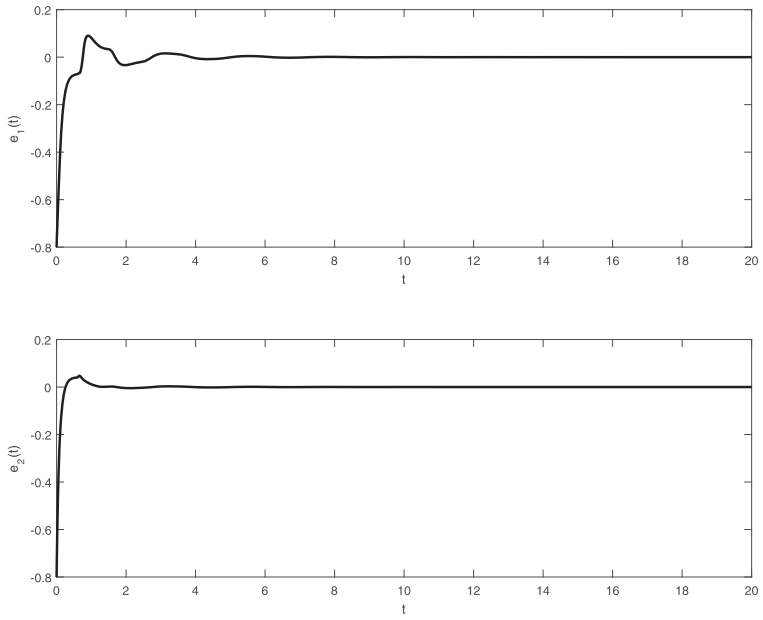

Fig. 16. The error curves of drive-response system (22) with the controller.

$$\sum_{j=1}^{2} b_{j1}^{m} - \mu_1 = -2.3 < 0,$$

$$\sum_{j=1}^{2} b_{j2}^{m} - \mu_2 = -2.9 < 0.$$

Obviously, all the parameters in Eq. (22) satisfy the conditions (19). Figs. (14)–(16) show the phase diagram, trajectories and error curves of the drive-response system (22) with controller (10), respectively.

Finally, we calculate the synchronization settling time of the system (22). In virtue of the controller (10), we have $\lambda = 1, \theta = 2, \iota = 1.2$ and $T_{max} = 6.0$.

Remark 11. *Example 2* is used to verify the validity of the results in Corollary 2, which aims at the fixed-time synchronization for MFCNN without time-varying delays. And *Example 3* is to verify the results of Corollary 3, which is used to dealing with the fixed-time synchronization for memristor-based neural networks with time-varying and without fuzzy logic. The simulation results show the effectiveness of **Corollaries 2** and **3**.

5. Conclusion and future work

The fixed-time synchronization problem of the drive-response MFCNN is investigated based on the definitions of fixed-time stability and fixed-time synchronization. With the help of dif-

ferential inclusion, set-valued map and inequality technology, we derive novel sufficient conditions for the drive and response systems to achieve fixed-time synchronization by defining a simple Lyapunov function and a nonlinear feedback controller. The proof process is concise and synchronization criteria are easily verifiable. Moreover, the main results of this paper can be extended to the MFCNN without time-varying delay and general memristor-based neural networks. The settling time of fixed-time synchronization can be easily calculated. Finally, three simulation examples show the effectiveness of our results.

It is worth pointing out that the existence of impulses has an important effect on synchronization. In [62], Zhang et al. studied exponential synchronization of coupled switched neural networks with mode-dependent impulsive effects, which is a new concept of impulse. But the processing of the switch in [62] is different from the memristor-based neural network in our paper. In [63], there was investigated synchronization problem of dynamical networks with heterogeneous impulses. Based on these well-studied results, a variety of impulses will be a problem to be considered in our future work. Moreover, further work also includes the following aspects: (1)Further analysis of the dynamical behavior of the MFCNN with various types of delays, such as distributed delay, leakage delay, neutral delay, etc.; (2) How to analyze the fixed-time stability and synchronization problems of the MFCNN when it includes noise and stochastic perturbations? In a word, the MFCNN still has some open problems.

References

[1] L.O. Chua, L. Yang, Cellular neural networks: theory, IEEE Trans. Circ. Syst. 35 (10) (1988) 1257–1272.

[2] J. Kung, D. Kim, S. Mukhopadhyay, On the impact of energy-accuracy tradeoff in a digital cellular neural network for image processing, IEEE Trans. Comput. Aided Des. Integr. Circ. Syst. 34 (7) (2015) 1070–1081.

[3] J.C. Chedjou, K. Kyamakya, A universal concept based on cellular neural networks for ultrafast and flexible solving of differential equations, IEEE Trans. Neural Netw. Learn. Syst. 26 (4) (2015) 749–762.

[4] A.R. Trivedi, S. Datta, S. Mukhopadhyay, Application of silicon-germanium source tunnel-FET to enable ultralow power cellular neural network-based associative memory, IEEE Trans. Electron Devices 61 (11) (2014) 3707–3715.

[5] N. Zeng, Z. Wang, B. Zineddin, Y. Li, M. Du, L. Xiao, X. Liu, T. Young, Image-based quantitative analysis of gold immunochromatographic strip via cellular neural network approach, IEEE Trans. Med. Imag. 33 (5) (2014) 1129–1136.

[6] B. Zineddin, Z. Wang, X. Liu, Cellular neural networks, the Navier–Stokes equation, and microarray image reconstruction, IEEE Trans. Image Process. 20 (11) (2011) 3296–3301.

[7] K. Kim, S. Lee, J.-Y. Kim, M. Kim, H.-J. Yoo, A configurable heterogeneous multicore architecture with cellular neural network for real-time object recognition, IEEE Trans. Circ. Syst. Video Technol. 19 (11) (2009) 1612–1622.

[8] A. Baştürk, E. Günay, Efficient edge detection in digital images using a cellular neural network optimized by differential evolution algorithm, Expert Syst. Appl. 36 (2) (2009) 2645–2650.

[9] H. Magnussen, J.A. Nossek, L.O. Chua, The Learning Problem for Discrete-Time Cellular Neural Networks As a Combinatorial Optimization Problem, Electronics Research Laboratory, College of Engineering, University of California, 1993.

[10] A. Kellner, H. Magnussen, J.A. Nossek, Texture classification, texture segmentation and text segmentation with discrete-time cellular neural networks, in: Proceedings of the Third IEEE International Workshop on Cellular Neural Networks and their Applications, CNNA-94, IEEE, 1994, pp. 243–248.

[11] T. Yang, L.-B. Yang, Fuzzy cellular neural network: a new paradigm for image processing, Int. J. Circ. Theory Appl. 25 (6) (1997) 469–481.

[12] W. Shitong, W. Min, A new detection algorithm (NDA) based on fuzzy cellular neural networks for white blood cell detection, IEEE Trans. Inf. Technol. Biomed. 10 (1) (2006) 5–10.

[13] S. Wang, D. Fu, M. Xu, D. Hu, Advanced fuzzy cellular neural network: Application to CT liver images, Artif. Intell. Med. 39 (1) (2007) 65–77.

[14] C.-T. Lin, C.-M. Yeh, S.-F. Liang, J.-F. Chung, N. Kumar, Support-vector-based fuzzy neural network for pattern classification, IEEE Trans. Fuzzy Syst. 14 (1) (2006) 31–41.
[15] L. Chua, Memristor – the missing circuit element, IEEE Trans. Circ. Theory 18 (5) (1971) 507–519.
[16] D.B. Strukov, G.S. Snider, D.R. Stewart, R.S. Williams, The missing memristor found, Nature 453 (7191) (2008) 80–83.
[17] S.H. Jo, T. Chang, I. Ebong, B.B. Bhadviya, P. Mazumder, W. Lu, Nanoscale memristor device as synapse in neuromorphic systems, Nano Lett. 10 (4) (2010) 1297.
[18] M. Shahsavari, P. Falez, P. Boulet, Combining a volatile and nonvolatile memristor in artificial synapse to improve learning in spiking neural networks, in: Proceedings of the IEEE/ACM International Symposium on Nanoscale Architectures (NANOARCH), IEEE, 2016, pp. 67–72.
[19] Z. Wang, S. Joshi, S.E. Savelev, H. Jiang, R. Midya, P. Lin, M. Hu, N. Ge, J.P. Strachan, Z. Li, et al., Memristors with diffusive dynamics as synaptic emulators for neuromorphic computing, Nat. Mater. 16 (1) (2017) 101–108.
[20] K.J. Kuhn, Considerations for ultimate CMOS scaling, IEEE Trans. Electron Dev. 59 (7) (2012) 1813–1828.
[21] Y. Zhang, X. Wang, Y. Li, E.G. Friedman, Memristive model for synaptic circuits, IEEE Trans. Circ. Syst. II Expr. Briefs 64 (7) (2017) 767–771.
[22] S. Kvatinsky, E.G. Friedman, A. Kolodny, U.C. Weiser, Team: threshold adaptive memristor model, IEEE Trans. Circ. Syst. I Reg. Pap. 60 (1) (2013) 211–221.
[23] D. Soudry, D. Di Castro, A. Gal, A. Kolodny, S. Kvatinsky, Memristor-based multilayer neural networks with online gradient descent training, IEEE Trans. Neural Netw. Learn. Syst. 26 (10) (2015) 2408–2421.
[24] S. Choi, P. Sheridan, W.D. Lu, Data clustering using memristor networks, Sci. Rep. 5 (2015) 10492.
[25] M. Prezioso, F. Merrikh-Bayat, B.D. Hoskins, G.C. Adam, K.K. Likharev, D.B. Strukov, Training and operation of an integrated neuromorphic network based on metal-oxide memristors, Nature 521 (7550) (2015) 61–64.
[26] Y.V. Pershin, S. La Fontaine, M. Di Ventra, Memristive model of amoeba learning, Phys. Rev. E 80 (2) (2009) 021926.
[27] I. Gupta, A. Serb, A. Khiat, R. Zeitler, S. Vassanelli, T. Prodromakis, Real-time encoding and compression of neuronal spikes by metal-oxide memristors, Nat. Commun. 7 (2016) 12805.
[28] L.M. Pecora, T.L. Carroll, Synchronization in chaotic systems, Phys. Rev. Lett. 64 (8) (1990) 821.
[29] G. Kamenkov, On stability of motion over a finite interval of time, J. Appl. Math. Mech. 17 (2) (1953) 529–540.
[30] A. Polyakov, Nonlinear feedback design for fixed-time stabilization of linear control systems, IEEE Trans. Autom. Control 57 (8) (2012) 2106–2110.
[31] A. Muralidharan, R. Pedarsani, P. Varaiya, Analysis of fixed-time control, Transp. Res. Part B Methodol. 73 (2015) 81–90.
[32] Y. Ma, T. Houghton, A. Cruden, D. Infield, Modeling the benefits of vehicle-to-grid technology to a power system, IEEE Trans. Power Syst. 27 (2) (2012) 1012–1020.
[33] Q. Xiao, Z. Zeng, Scale-limited lagrange stability and finite-time synchronization for memristive recurrent neural networks on time scales, IEEE Trans. Cybern. 47 (10) (2017) 2984–2994.
[34] X. Liu, J. Cao, W. Yu, Q. Song, Nonsmooth finite-time synchronization of switched coupled neural networks, IEEE Trans. Cybern. 46 (10) (2016) 2360–2371.
[35] X. Liu, H. Su, M.Z.Q. Chen, A switching approach to designing finite-time synchronization controllers of coupled neural networks, IEEE Trans. Neural Netw. Learn. Syst. 27 (2) (2016) 471–482.
[36] X. Yang, D.W.C. Ho, J. Lu, Q. Song, Finite-time cluster synchronization of T–S fuzzy complex networks with discontinuous subsystems and random coupling delays, IEEE Trans. Fuzzy Syst. 23 (6) (2015) 2302–2316.
[37] M. Zheng, L. Li, H. Peng, J. Xiao, Y. Yang, H. Zhao, Finite-time stability analysis for neutral-type neural networks with hybrid time-varying delays without using Lyapunov method, Neurocomputing 238 (2017) 67–75.
[38] M. Zheng, L. Li, H. Peng, J. Xiao, Y. Yang, H. Zhao, Finite-time stability and synchronization for memristor-based fractional-order Cohen–Grossberg neural network, Eur. Phys. J. B 89 (9) (2016) 204.
[39] A. Polyakov, D. Efimov, W. Perruquetti, Finite-time and fixed-time stabilization: implicit Lyapunov function approach, Automatica 51 (2015) 332–340.
[40] Y. Wan, J. Cao, G. Wen, W. Yu, Robust fixed-time synchronization of delayed Cohen–Grossberg neural networks, Neural Netw. 73 (2016) 86–94.
[41] W. Lu, X. Liu, T. Chen, A note on finite-time and fixed-time stability, Neural Netw. 81 (2016) 11–15.
[42] X. Liu, T. Chen, Finite-time and fixed-time cluster synchronization with or without pinning control, IEEE Trans. Cybern. 48 (1) (2018) 240–252.
[43] Z. Xing, J. Peng, Exponential lag synchronization of fuzzy cellular neural networks with time-varying delays, J. Frankl. Inst. 349 (3) (2013) 1074–1086.

[44] Q. Gan, R. Xu, P. Yang, Synchronization of non-identical chaotic delayed fuzzy cellular neural networks based on sliding mode control, Commun. Nonlinear Sci. Numer. Simul. 17 (1) (2012) 433–443.
[45] A. Abdurahman, H. Jiang, Z. Teng, Finite-time synchronization for fuzzy cellular neural networks with time–varying delays, Fuzzy Sets Syst. 297 (2016) 96–111.
[46] C. Huang, D.W.C. Ho, J. Lu, J. Kurths, Pinning synchronization in TCS fuzzy complex networks with partial and discrete-time couplings, IEEE Trans. Fuzzy Syst. 23 (4) (2015) 1274–1285.
[47] J. Lu, C. Ding, J. Lou, J. Cao, Outer synchronization of partially coupled dynamical networks via pinning impulsive controllers, J. Frankl. Inst. 352 (11) (2015) 5024–5041.
[48] Y. Wan, J. Cao, Periodicity and synchronization of coupled memristive neural networks with supremums, Neurocomputing 159 (2015) 137–143.
[49] W. Wang, C. Huang, J. Cao, F.E. Alsaadi, Event-triggered control for sampled-data cluster formation of multi--agent systems, Neurocomputing 267 (2017) 25–35.
[50] H. Lu, Chaotic attractors in delayed neural networks, Phys. Lett. A 298 (2) (2002) 109–116.
[51] X. Yang, J. Cao, J. Qiu, Pth moment exponential stochastic synchronization of coupled memristor-based neural networks with mixed delays via delayed impulsive control, Neural Netw. 65 (2015) 80–91.
[52] H. Wu, X. Han, L. Wang, Y. Wang, B. Fang, Exponential passivity of memristive neural networks with mixed time-varying delays, J. Frankl. Inst. 353 (3) (2016) 688–712.
[53] A.F. Filippov, Differential equations with discontinuous right-hand side, Matematicheskii sbornik 93 (1) (1960) 99–128.
[54] A.F. Filippov, Differential Equations with Discontinuous Righthand Sides: Control Systems, 18, Springer Science & Business Media, 2013.
[55] J.P. Aubin, A. Cellina, Differential Inclusions: Set-Valued Maps and Viability Theory, Springer-Verlag New York, Inc., 1984.
[56] C. Hu, J. Yu, Z. Chen, H. Jiang, T. Huang, Fixed-time stability of dynamical systems and fixed-time synchronization of coupled discontinuous neural networks, Neural Netw. 89 (2017) 74–83.
[57] T. Yang, L.-B. Yang, The global stability of fuzzy cellular neural network, IEEE Trans. Circ. Syst. I Fundam. Theory Appl. 43 (10) (1996) 880–883.
[58] H.K. Khalil, J. Grizzle, Nonlinear Systems, third ed., Prentice Hall, Upper Saddle River, 2002.
[59] J. Chen, Z. Zeng, P. Jiang, Global Mittag–Leffler stability and synchronization of memristor-based fractional-order neural networks, Neural Netw. 51 (2014) 1–8.
[60] J. Cao, R. Li, Fixed-time synchronization of delayed memristor-based recurrent neural networks, Sci. Chin. Inf. Sci. 60 (3) (2017) 032201.
[61] L. Wang, Z. Zeng, J. Hu, X. Wang, Controller design for global fixed-time synchronization of delayed neural networks with discontinuous activations, Neural Netw. 87 (2017) 122–131.
[62] W. Zhang, Y. Tang, Q. Miao, W. Du, Exponential synchronization of coupled switched neural networks with mode-dependent impulsive effects, IEEE Trans. Neural Netw. Learn. Syst. 24 (8) (2013) 1316–1326.
[63] W. Zhang, Y. Tang, X. Wu, J.A. Fang, Synchronization of nonlinear dynamical networks with heterogeneous impulses, IEEE Trans. Circ. Syst. I Reg. Pap. 61 (4) (2017) 1220–1228.